UNIVERSITY OF CALIFORNIA
RIVERSIDE

Characterization of Drought Hydraulic Strategies of Neotropical Lowland Forests

A Dissertation submitted in partial satisfaction
of the requirements for the degree of

Doctor of Philosophy

in

Evolution, Ecology and Organismal Biology

by

Mark Eric De Guzman

June 2017

Dissertation Committee:
Dr. Louis S. Santiago, Chairperson
Dr. Anna L. Jacobsen
Dr. Amy Litt

The Dissertation of Mark Eric De Guzman is approved:

_____

_____

_____

Committee Chairperson

University of California, Riverside

ACKNOWLEDGMENTS

The first chapter on comparative hydraulic between liana and tree species has been published through Oxford University Press with the title "Trade-offs between water transport capacity and drought resistance in neotropical canopy liana and tree species," the article was authored by Mark E. De Guzman, Louis S. Santiago, Stefan A. Schnitzer, and Leonor Álvarez-Cansino in 2016 in the journal Tree Physiology with the doi: 10.1093/treephys/tpw086. I gratefully acknowledge Eric Manzané for valuable support in the field; Eric Díaz for technical assistance in the field; Crane operators Edwin Andrade and Julio Pitti for maneuvering us to measurement branches; Owen McMillan, Nelida Gomez and Adrianna Bilgray from the Smithsonian Tropical Research Institute (STRI), Office of Academic Programs for logistical support; Klaus Winter of STRI generous use of lab space; Milton Garcia for expert knowledge and technical support; Brett Wolfe and Thomas Kursar of the University of Utah for use of their thermocouple psychrometer; Anna Jacobsen for methodological support with standard centrifuge method; Christopher Baraloto, Damien Bonal and Claire Fortunel of Institut National de la Recherche Agronomique for helpful discussions; Eleinis A. Ávila-Lovera for assistance; The anonymous referees and Santiago lab group who provided comments which help to improve the quality of this manuscript. The University of California, Department of Botany & Plant Sciences and Marquette University, Department of Biological Sciences are thanked for logistical support. This work conforms to the legal requirements of the country in which it was carried out. This work was funded by the STRI Introduction to Neotropical Research and Culture Internship Program to Mark E. De Guzman, National

Science Foundation awards (DEB 0845071 and DEB 1019436) to Stefan A. Schnitzer, and National Science Foundation award (IOS 0817212) to Louis S. Santiago.

The second chapter was made possible due to the help of the various collaborators including Damien Bonal, Christopher Baraloto, Bruno Hérault, Claire Fortunel, Jacob E. Vogenberg, and Max A. Brodie. I graciously acknowledge Benoît Burban and Jean-Yves Goret for laboratory support, Jocelyn Cazal and Valentine Alt for skillfully climbing trees for samples, Aurelie Dourdain for database support, and Clement Stahl for discussion on the data presented. I also acknowledge the University of California Department of Botany & Plant Sciences for support. Funding for fieldwork and data acquisition was provided by Investissement d'Avenir grants of the French ANR (CEBA: ANR-10-LABx-0025), through the "DRAMA" and "HydroSTAT" projects. Funding for part of this work was also provided by Devirian Graduate Research Award and Labex-CEBA Thematic School on "Functional Ecology of Tropical Rainforests in the Context of Climate Changes: From Real Observations to Simulations."

The third chapter was made possible through the help of my collaborators Gaspar Silvera, Ministerio de Desarrollo Agropecuario (MIDA) for administering the agricultural experiment, and STRI for logistical support in Panama. Klaus Winter of STRI is thanked for generous use of lab space; Milton Garcia for expert knowledge and technical support. I also acknowledge the University of California Department of Botany & Plant Sciences for providing support. Funding for fieldwork and data acquisition was provided by the USDA National Institute for Food and Agriculture.

I would like to thank various mentors who have helped me get to this stage. I would like to acknowledge Carl Kloock, Brandon Pratt, Anna Jacobsen, and Isabel Sumaya from my college days at CSU Bakersfield for preparing me for graduate studies. I would like to thank Kurt Anderson, Edith Allen, Jeff Diez, Matthew Dougherty, Darrel Jenerette, Carol Lovatt, and James Sickman at UCR for their help and valuable input in my graduate education.

I would like to acknowledge the University of California, Biology Department graduate program and the Evolution, Ecology and Organismal Biology program for supporting me through these years. I would also like to acknowledge additional funding sources including the Dean's Distinguished Fellowship Award, Caliche project, and NSF Rapid grant that supported me financially through the graduate program. I would like to acknowledge Melissa Gomez and Amy S. Ricks for their phenomenal logistical support. I would like to acknowledge my cohort for helping me realize a good work and life balance as I went through the rigors of the graduate study. I would like to acknowledge members of the Santiago Lab Group including Aleyda Acosta-Rangel, Eleinis Ávila-Lovera, Max A. Brodie, Manika Choudhary, Dr. Mustapha Gorai, Roxana Haro, Obaid Khan, Brandon McNellis, Sarah Pasquini, Alexandria Pivovaroff, Yong Shen, Luis Torres, Michael Torres, Dr. Angela Vitoria, Jacob E. Vogenberg, Victoria Woods, and Larissa Yates for their encouragements and support through the years.

DEDICATION

As I write in the warm embrace of the tropical forest of Panama, a delicate but potent feeling of nostalgia reminded me of the phrase that encapsulates my appreciation for the blessings I received:

"And, when you want something, all the universe conspires in helping you to achieve it."

- Paulo Coelho, The Alchemist

The many conspirators that the universe sent my way helped me through the arduous journey of learning how to use tools to peer into the processes that surround us in our daily lives. Through this segment of my life, I became more aware not only of the beauty of life but also its transiency. I owe so much to the universe's conspirators that not only enabled me to learn and appreciate the life around me, but also helped further sculpt my ideas and identity.

I dedicate this dissertation to my family and friends who helped me along the way. To my grandparents, I thank you all for the love and support all my life. To my parents Ernesto and Donna, I am deeply thankful for having wonderful parents! The loving environment you have provided us siblings ranging from the comfortable home, outstanding schools, and a future full of opportunities to name a few have made my life to date fulfilling. I know that both of you made many personal and career sacrifices, some of which weighs heavily, and made me feel your endless love. More than anyone else, both of you helped mold me to what I am today. To my sister Marie, you always had a knack for knowing what I needed and being there when I needed it the most, so thank you. To my brothers Erwin and Tim, as the honorary triplet I thank you for being always there for me and helping me relax from the stresses of graduate life. To my friend Karl

Umali, thank you for being there to talk about life despite being literally halfway around the world. To Aaron Ramirez and Gilberto Uribe, thank you for memorable times in college and graduate school. Your insights and company helped un-complicate life while making it ridiculously fun.

ABSTRACT OF THE DISSERTATION

Characterization of Drought Hydraulic Strategies
of Neotropical Lowland Forests

by

Mark Eric De Guzman

Doctor of Philosophy, Graduate Program in Evolution, Ecology and Organismal Biology
University of California, Riverside, June 2017
Dr. Louis S. Santiago, Chairperson

The struggles of Angiosperms to deal with the challenges of the vertical ascent of sap have led to the diverse hydraulic strategies that we see among plants today. Different strategies of hydraulic transport are multifaceted and coordinated among organs and are highly attuned to different environments, which promotes effective resource acquisition and utilization. In light of the climate changes occurring in the Anthropocene, the plant hydraulic strategies will dictate which plants will tolerate drought and which plants will succumb to drought and ultimately to mortality. A framework to explain plant mortality has been recently proposed where a trade-off exists between plants that utilize profligate hydraulic strategies but are vulnerable to hydraulic failure and plants that utilize conservative hydraulic strategies but are vulnerable to carbon starvation. Currently, the information on the physiological traits that are most useful in modeling and successfully

predicting plant mortality is limited. Identifying key hydraulic traits is important in increasing predictive power in modeling future tropical forest composition and dynamics. The goal of this dissertation was to characterize the hydraulic physiological traits that underpin plant drought response strategies by utilizing plant hydraulic research methods to describe hydraulic architecture and capacities in transport, storage and resistance to dysfunction (i.e. cavitation resistance). Furthermore, these traits were used in conjunction with other techniques that describe how carbon and nutrient dynamics vary such as gas exchange and stable isotopes measures. This dissertation provides information on a potential physiological mechanism driving the observed increase in liana abundance in tropical forests, proposes a novel drought response trait in the ability to form vessel occlusions and the relationship of vessel occlusions to other hydraulic and anatomical traits, and applies this information from natural systems to assess physiological performance of avocado varieties.

Table of Contents

List of Figures

List of Tables

Introduction

The aim of the experimental field of plant ecophysiology is to characterize the physiological mechanisms underlying ecological observations. Plant ecophysiology attempts to answer questions derived from ecology, such as patterns of plant distribution relative to the environment, by providing detailed physiological mechanisms as the basis for explanation (Lambers *et al.* 2008). Lambers *et al.* (2008) explained that observations of differences in morphological traits of plants by geographers (Schimper 1903, Warming 1909) and the desire to learn how plants respond to environmental stresses for agricultural benefit (Boyer 1985) provided the impetus for the development of the field of plant ecophysiology. Typically, this field employs techniques that measure the microenvironment, water relations, and carbon dynamics of the plants, and this provides a mechanistic understanding of why and how plants are able to grow where they do. Furthermore, these measures create the capability to predict how plants may respond to shifting environmental conditions (Holdridge 1947) and also generate quantitative values that can be extrapolated to the processes happening at higher levels of organization (Lambers *et al.* 2008). It is important to note that ecophysiology is used at levels of organization ranging from the biochemical pathways of cells and tissues to large scale ecosystem fluxes.

References

Boyer JS. 1985. Water transport. *Annual Review of Plant Physiology* **36**: 473-516.

Holdridge LR. **1947**. Determination of world plant formations from simple climatic data. *Science* **105**: 367-368.

Lambers H, Chapin III FS, and Pons TL. **2008**. *Plant Physiological Ecology*. Springer Verlag, New York, USA.

Schimper AFW eds. Groom P and Balfour IB. **1903**. *Plant-Geography Upon A Physiological Basis*, Clarendon Press, Oxford, England.

Warming E. **1909**. *Oecology of Plants*, Clarendon Press, Oxford, England.

Chapter 1

Trade-offs between water transport capacity and drought resistance in neotropical canopy liana and tree species

Published as: De Guzman ME, Santiago LS, Schnitzer S, Álvareze-Cansino L. 2016. Trade-offs between water transport capacity and drought resistance in neotropical canopy liana and tree species. *Tree Physiology* doi:10.1093/treephys/tpw086

Abstract

In tropical forest canopies, it is critical for upper shoots to efficiently provide water to leaves for physiological function while safely preventing loss of hydraulic conductivity due to cavitation during periods of soil water deficit or high evaporative demand. We compared hydraulic physiology of upper canopy trees and lianas in a seasonally dry tropical forest to test whether trade-offs between safety and efficiency of water transport shape differences in hydraulic function between these two major tropical woody growth forms. We found that lianas showed greater maximum stem-specific hydraulic conductivity than trees, but lost hydraulic conductivity at less negative water potentials than trees, resulting in a negative correlation and trade-off between safety and efficiency of water transport. Lianas also exhibited greater diurnal changes in leaf water potential than trees. The magnitude of diurnal water potential change was negatively correlated with sapwood capacitance, indicating that lianas are highly reliant on conducting capability to maintain leaf water status, whereas trees relied more on stored water in stems to maintain leaf water status. Leaf nitrogen concentration was related to maximum leaf-specific hydraulic conductivity only for lianas suggesting that greater water transport capacity is more tied to leaf processes in lianas compared to trees. Our results are consistent with a trade-off between safety and efficiency of water transport and may have implications for increasing liana abundance in neotropical forests.

Introduction

A current paradigm in plant hydraulics suggests a major tradeoff between two indices of hydraulic function: maximum water transport capacity per unit cross-sectional sapwood area (K_S), or hydraulic efficiency, and resistance to drought-induced xylem cavitation, or hydraulic safety (Pockman & Sperry, 2000; Martínez-Vilalta *et al.*, 2002). This tradeoff is considered to be a major axis of plant strategy variation (Ackerly, 2004; Choat *et al.*, 2012), and is related to dynamic indices of hydraulic function including water acquisition, regulation of water use and water-use efficiency (Drake and Franks 2003, Santiago et al. 2004b, Bucci et al. 2009, Meinzer et al. 2009). A recent analysis across a broad range of species, including 335 angiosperms and 89 gymnosperms suggests that globally, this relationship is significant, but weak, and that although there are no species with both safe and efficient hydraulic systems, the numerous species with low efficiency and low safety presents a curious conundrum to this paradigm (Gleason *et al.*, 2015). Yet, correlations among traits at the global scale does not necessarily mean that the same relationships operate in regional or site-specific data sets (Santiago & Wright, 2007). Within-site trait relationships likely reflect local resource availability and the identity of taxa that are present. Indeed, strong trade-offs between safety and efficiency have been observed within numerous single sites (Pockman & Sperry, 2000; Martínez-Vilalta *et al.*, 2002; Pratt *et al.*, 2007) and among particular taxa (Wheeler *et al.*, 2005; Hacke *et al.*, 2007). We used this context to examine hydraulic differences between trees and lianas, the two main woody growth forms of tropical forest.

The safety-efficiency trade-off in plants is based on hydraulic theory and data demonstrating that the maximum rate of water flow through xylem vessels increases with the diameter of the vessel, and that wider vessels often cavitate at less negative water potentials than narrower vessels (Pockman & Sperry, 2000; Martínez-Vilalta *et al.*, 2002; Wheeler *et al.*, 2005). The vulnerability of large diameter vessels to freezing-induced cavitation is substantially increased (Tyree *et al.*, 1994). However, for tropical plants, safety from cavitation by water stress is a greater constraint to vessel size than freezing. The pit area hypothesis suggests an increasing probability of the seal of inter-vessel pits failing as the total area of pits increases (Wheeler *et al.*, 2005). The result is a complex trade-off between vessel size and vulnerability to cavitation by water stress that is too variable to allow physiologists to predict vulnerability to drought-induced cavitation based on vessel diameter, but strong enough to constrain xylem function to a limited range of operation (Tyree *et al.*, 1994; Hacke *et al.*, 2006; Sperry *et al.*, 2008; Gleason *et al.*, 2015).

Relatively little data comparing lianas and trees exist for the trade-off between K_S and vulnerability to xylem cavitation (Santiago *et al.*, 2015). The emerging pattern suggests that lianas and trees fall along the same relationship of hydraulic safety versus efficiency, but that lianas show a tendency for greater maximum stem-specific conductivity and a less resistant xylem, and thus occupy the relatively less safe and more efficient side of the spectrum (Zhu & Cao, 2009; Johnson *et al.*, 2013; van der Sande *et al.*, 2013; Santiago *et al.*, 2015). If this pattern is robust, it would appear that the enhanced ability to transport water and support photosynthesis of canopy leaves may be

more important than drought resistance in determining liana success. Reports generated through a variety of metrics indicate that the slender stems of lianas normally support a distal leaf area that is considerably greater than trees when normalized per unit stem area (Putz, 1993; Gerwing & Farias, 2000; Restom & Nepstad, 2001; Feild & Balun, 2008; Zhu & Cao, 2009). There is also some evidence that lianas exhibit greater average stem-specific hydraulic conductivity than trees (Gartner *et al.*, 1990; Patiño *et al.*, 1995), supporting the idea that lianas utilize wide vessels to maintain efficient water transport to compensate for narrow stems (Ewers & Fisher, 1991). Patterns of leaf-specific hydraulic conductivity (K_L) between lianas and trees, on the other hand, show more variation. For example, the studies of Feild and Balun (2008) and Zhu and Cao (2009) show lower K_L in lianas relative to trees. However, Patiño et al. (1995) and Santiago et al. (2015), both of which reviewed several studies, show higher K_L in lianas relative to trees. These data suggest that in general, greater water transport capacity in lianas promotes higher leaf photosynthetic potential than trees as has been observed in some studies (Zhu & Cao, 2009, 2010; Asner & Martin, 2012), indicating that interactions between water supply to leaves and photosynthetic carbon gain may be a critical component of the liana strategy.

It is well established that hydraulic efficiency controls maximum stomatal conductance (Meinzer and Grantz 1990, Meinzer et al. 1995, Pockman and Sperry 2000, Hubbard et al. 2001, Santiago et al. 2004a). Because stomatal conductance promotes CO_2 diffusion to the site of carboxylation, plants are expected to allocate to relatively greater photosynthetic capacity as water supply to leaves increases in order to take advantage of a high supply of CO_2 for photosynthesis (Santiago et al. 2004a) Therefore, hydraulically

efficient plant species are also predicted to occur on the fast-return on investment side of the leaf economics spectrum, including high rates of maximum photosynthesis, high leaf element concentrations and high specific leaf area, whereas species with low hydraulic efficiency are predicted to exhibit opposite traits (Wright *et al.*, 2004b; Maire *et al.*, 2015). Further linkages between stem and leaf coordination of hydraulic processes are evident in stable isotopic composition of carbon ($\delta^{13}C$) and nitrogen ($\delta^{15}N$) in leaves. Leaf $\delta^{13}C$ is related to intercellular CO_2 concentration (C_i) such that high rates of stomatal conductance are often associated with high C_i, high rates of discrimination by rubisco against $^{13}CO_2$ relative to $^{12}CO_2$, and low values of $\delta^{13}C$ (Farquhar *et al.*, 1982). Leaf $\delta^{15}N$ in non N_2-fixing species is related to the transpiration efficiency of N acquisition because nitrate reductase in the root preferentially reduces $^{14}NO_3^-$, leading to a pool enriched in ^{15}N that is transported to shoots through the transpiration stream (Cernusak *et al.*, 2009). Thus hydraulic efficiency has implications for water, carbon and nutrient relations of leaves and appears to function as an overall constraint to leaf metabolic processes.

Trees and lianas are the two major woody growth forms in tropical forests, but several reports, mostly from the neotropics, indicate that the relative abundance of lianas compared to trees is increasing (Phillips *et al.*, 2002; Wright *et al.*, 2004a; Chave *et al.*, 2008; Schnitzer & Bongers, 2011; Laurance *et al.*, 2014). Although increasing disturbance and forest fragmentation have been implicated in this change (Schnitzer & Bongers, 2011), many of the reports of increasing liana abundance pertain to undisturbed or mature forest (Schnitzer & Bongers, 2011; Laurance *et al.*, 2014). Furthermore, other

hypotheses to explain the relatively sudden increase in relative abundance of neotropical lianas include changes in precipitation patterns (Schnitzer & Bongers, 2011; Schnitzer *et al.*, 2015). Thus differences in the hydraulic function of trees and lianas could have important implications for the competitive balance between these two growth forms during climate change. We sought to compare the hydraulic physiology of upper canopy trees and lianas in a seasonally dry tropical forest to test whether trade-offs between safety and efficiency of water transport shape differences in hydraulic function between these two major tropical woody growth forms. Our main study questions were: How do stem hydraulic traits and wood biophysical properties differ between trees and lianas? Is there evidence of a trade-off between safety and efficiency of water transport? What are the relationships between leaf water usage and stem hydraulic traits? How do hydraulic traits affect leaf chemistry and photosynthetic potential?

Materials and Methods

Study site and species

The study was conducted in a lowland tropical forest in Parque Natural Metropolitano, Panamá (8°59'N, 79°33'W). The site is a seasonally dry semi-deciduous forest with wet seasons occurring between May and November and a mean annual precipitation of 1865 mm. The soils are well-drained clays and composed of volcanic substrate (Santiago et al. 2004b). Measurements were conducted on six tree species and six liana species (Table 1.1) accessible from a canopy crane maintained by the Smithsonian Tropical Research Institute (STRI). The crane is equipped with a gondola suspended by cables from a rotating arm that enables access to approximately 0.85 ha of forest and 30-40 m canopy height. Measurements were made between 1 June and 8 September 2012, during the early and mid-wet season. All species were sampled at the top of the canopy. For each species, we measured six individuals except *Cordia alliodora* (Ruiz & Pav.) Cham. ex A. DC., which has only three individuals accessible from the crane.

Water potential and stomatal conductance

Three upper canopy leaves with full sun exposure from three individuals per species were cut at the petiole and then immediately bagged and stored in a dark cooler to prevent further transpiration. Sampling occurred between 1100 and 1300 h for midday bulk leaf water potential ($\Psi_{leaf\ md}$; MPa) and between 0330 and 0630 h for pre-dawn bulk leaf water potential ($\Psi_{leaf\ pd}$; MPa) on the same branches, and measurements were

stratified among species in three rounds to avoid bias in timing of measurement. Measurements of $\Psi_{leaf\,md}$ and $\Psi_{leaf\,pd}$ were determined within 10 minutes of collection using a Scholander pressure chamber (Model 600D; Plant Moisture Stress Instruments, Albany, OR, USA). The diurnal range of Ψ_{leaf} ($\Delta\Psi_{leaf}$) was calculated from the difference between $\Psi_{leaf\,md}$ and $\Psi_{leaf\,pd}$. Maximum stomatal conductance ($g_{s\,max}$) was measured with a steady-state porometer (SC-1 Leaf Porometer; Decagon Devices, Pullman, WA, USA) between 0900 – 1100 h.

Stem hydraulic conductivity, vulnerability curve, and safety margin

One sun exposed terminal branch (1.0 – 2.5 m in length) from each individual was collected from the top of the canopy between 0700 and 0900 h for measurements of hydraulic parameters. Cut ends of branches were sealed with parafilm and immediately placed in two layers of opaque plastic bags with moist paper towels to prevent further transpiration. Samples were transported to the STRI Earl S. Tupper Facility in Ancón, Panama within one hour. In the laboratory, the recently collected 1.0 cm diameter stems were cut under water to a length of 20 cm. Liana samples were cut to include an internode and two nodes located between the cut ends (Jacobsen & Pratt, 2012). Stem hydraulic conductivity (K_H; kg m s^{-1} MPa^{-1}) was measured by connecting the stem to tubing filled with a degassed 20 mM KCl perfusion solution filtered through a 0.1 micron capsule filter (GE Water & Process Technologies, Trevose, PA, USA), with the basal end connected to an elevated fluid reservoir and the terminal end connected to a 1-ml pipette (KIMAX-51; Kimble Chase, Vineland, NJ, USA) to determine the flow rate from

changes in volume over time. The pressure head was maintained below 2 kPa to avoid refilling open vessels (Jacobsen & Pratt, 2012; Tobin *et al.*, 2013). Before and after measurement, background flow was measured for 5 minutes without a pressure head to confirm that no stem passive water uptake occurred (Torres-Ruiz *et al.*, 2012). K_H was measured as the pressure-driven flow divided by the pressure gradient (Sperry *et al.*, 1988). Native stem hydraulic conductivity ($K_{H\ native}$) was determined prior to removing emboli from stems. Stems ends were then cleanly shaved with a razor blade and the stem was cut to a standard sample length of 14.2 cm prior to determination of maximum K_H ($K_{H\ max}$), after emboli were removed by vacuum infiltration under filtered water for at least 12 hours.

Xylem vulnerability to cavitation was determined with vulnerability curves generated using the standard centrifugation method (Alder *et al.*, 1997), in which conductivity is measured outside the centrifuge between inducing negative xylem pressures using the centrifuge. Several studies have demonstrated that no long-vessel artefact occurs with the static centrifugation method (Sperry *et al.*, 2012; Jacobsen & Pratt, 2012; Tobin *et al.*, 2013; Hacke *et al.*, 2015). Maximum xylem vessel lengths among our study species varied from 22-140 cm (Johnson et al. 2013, Louis Santiago, unpublished data). Stems were mounted in a 14.2-cm-diameter custom rotor in a refrigerated centrifuge (Sorvall RC-5C; Thermo Fisher Scientific, Waltham, MA, USA) with stem ends submerged in the 20 mM KCl perfusion solution contained in L-shaped reservoirs. Foam cosmetic sponges were added to the L-shaped reservoirs to soak up excess solution to keep stem ends in contact with solution even when the rotor was not

spinning (Jacobsen & Pratt, 2012; Tobin *et al.*, 2013; Hacke *et al.*, 2015). The solution volume in each reservoir was maintained at the same volume to prevent induction of flow during centrifugation. K_H was measured after each spin and the process was repeated until >90% of stem K_H was lost.

We expressed K_H as sapwood-specific conductivity (K_S; kg m^{-1} s^{-1} MPa^{-1}), through normalizing values by sapwood area, calculated as the difference between xylem and pith cross-sectional area. We also expressed conductivity as leaf specific conductivity (K_L; kg m^{-1} s^{-1} MPa^{-1}) through normalizing values by total leaf area distal to the conducting stem. Accordingly, $K_{H\,max}$ was expressed as maximum sapwood-specific hydraulic conductivity ($K_{S\,max}$) and maximum leaf-specific conductivity ($K_{L\,max}$). Resistance to drought-induced xylem cavitation was expressed as P_{50}, the water potential at which 50 per cent loss of conductivity (PLC) occurs in vulnerability curves. Hydraulic safety margins were derived from the vulnerability to cavitation curve following Meinzer et al. (2009) where the air entry threshold (P_e) is calculated as the *x*-intercept of the line tangent to P_{50}. The change in PLC after P_e is reached was calculated as P_e–P_{50}, where high values indicate a more gradual increase in PLC when xylem water potential falls below P_e. Leaf area to sapwood area ratio (LA:SA) was calculated by dividing the total leaf area distal to the conducting stem by the sapwood area.

Xylem capacitance and wood biophysical properties

Stem samples 0.5 m long and 0.5 – 1.5 cm in diameter were collected from study individuals between 0700 and 0900 h. One subsample was immediately separated for

measurement of native stem water potential ($\Psi_{stem\ native}$) in a thermocouple psychrometer chamber (83-1V Large Chamber Thermocouple Psychrometer; Merrill Instruments, Logan, UT, USA) connected to a data logger (PSΨPRO; Wescor, Logan, UT, USA), whereas the rest of the branch was re-cut under water to a length of 20 cm and rehydrated overnight. For measurement of xylem water potential (Ψ_x), stem samples were cut to 3 cm segments under water, the bark and pith were removed, samples were blotted with a paper towel, weighed on an analytical balance (Sartorius AG, Goettingen, Germany) to determine saturated mass, and immediately sealed in a thermocouple psychrometer chamber (83-3VC, Merrill Instruments). Three to six segments were used for each species to fill psychrometric chambers. The psychrometer chambers were allowed to equilibrate in an insulated water bath at room temperature (24 °C) for about 4 h, which was the amount of time to reach the first stable reading. Ψ_x was measured in psychrometric mode using an automated multi-channel microvoltmeter (CR7; Campbell Scientific, Logan, UT). After the determination of Ψ_x, the psychrometer chambers were removed from the water bath, partially dehydrated in a 40 °C oven, re-weighed, resealed in psychrometer chambers, and re-equilibrated in chambers for the next determination of Ψ_x. This was repeated seven to ten times until the tissue reached Ψ_x values of –3.0 to –7.0 MPa depending on the species. Following final determination of Ψ_x, samples were dried at 100 °C for 1 hour and then at 60 °C for 48 h and weighed to calculate tissue dry mass and water released. Capacitance (C; kg m^{-3} MPa^{-1}) was calculated as the slope of the near linear portion in the initial part of the xylem water release curve (Meinzer *et al.*, 2003, 2009). Wood density (ρ_{wood}) was calculated as dry mass divided by fresh tissue volume.

Leaf Traits and Chemistry

Samples of 1-10 young fully mature leaves, depending on the leaf sizes of different species, distal to the section used for hydraulic measurements were collected from each of the sample branches of each species. For measurement of specific leaf area (SLA; area divided by dry mass), 5-30 leaves were measured with an area meter and dried in an oven for 60°C for 48 h and weighed. For chemical analysis, leaves were placed in a coin envelope and dried in an oven at 60°C for 48 h. For large leaved species, intercostal tissue was collected between the mid-rib and the periphery at the centre of the leaf. Samples were ground and homogenized using a mill (8000D Dual Mixer/Mill; SPEX SamplePrep, Metuchen, NJ, USA). Homogenized samples of 1-2 mg were weighed and rolled in foil capsules. Samples were sent to the Facility for Isotope Ratio Mass Spectroscopy (FIRMS), University of California, Riverside, for analysis of total leaf nitrogen concentration (N), and isotopic composition of nitrogen ($\delta^{15}N$) and carbon ($\delta^{13}C$). Leaf N was expressed per unit leaf mass (N_{mass}) and per unit area (N_{area}) by dividing the mass-based values by SLA.

Statistical Analysis

Student's *t*-tests were used to evaluate differences of trait means between tree and liana species in *R* (R Core Team, 2016). Mann-Whitney *U* Tests were used for comparisons with non-normal distribution. We evaluated bivariate trait relationships with Pearson product-moment correlation using the Hmisc package in *R*. The leverage potential of *x*-

variable outliers was analysed with the hat matrix procedure (Neter *et al.*, 1990). Phylogenetic independent contrasts (PIC) were analysed using Phylocom (Webb *et al.*, 2009). Alpha was set at 0.05 for all comparisons. Normality tests were conducted prior to testing correlations. Non-normally distributed data were $\log_{10}$-transformed and absolute values were calculated prior to transformation for values that are normally reported as negative. Principal components analysis (PCA) was done with PAST statistical software (Hammer *et al.*, 2001), using the 21 physiological variables on the 12 canopy liana and tree species. We determined values for P_{50} using the best-fit non-linear regression to a Weibull function.

Results

We observed statistically significant variation between lianas and trees in 13 out of 21 physiological traits studied. Xylem vulnerability curves indicated that trees had more negative mean P_{50} values than lianas (Table 1.2), indicating greater resistance to drought-induced cavitation. Values for C were greater in trees than lianas (Table 1.2), indicating a greater ability to supply the water needed to limit rapid drops in water potential. However, water transport capacity expressed as $K_{S\ max}$, and $K_{L\ max}$ were significantly higher in lianas than in trees. Values for $K_{S\ native}$ were also greater in lianas than in trees, but values for $K_{L\ native}$ were statistically indistinguishable (Table 1.2).

Lianas experienced a greater daily change in water potential, with greater $\Delta\Psi_{leaf}$ than trees and this was driven by more negative $\Psi_{leaf\ md}$ and $\Psi_{stem\ native}$ in lianas, because there were no differences between trees and lianas for $\Psi_{leaf\ pd}$ (Table 1.2). There were no differences in air entry threshold (P_e), but hydraulic safety margin (P_e–P_{50}) was greater in trees than in lianas (Table 1.2). There was no difference between the two growth forms in $g_{s\ max}$ (Table 1.2). Lianas showed greater values of ρ_{wood} and LA:SA than trees, but had narrower terminal stem diameters (d_{branch}; Table 1.2). We also measured greater N_{area} in trees than in lianas, but there were no differences in $\delta^{15}N$, $\delta^{13}C$, N_{mass} or SLA (Table 1.2).

Vulnerability curves were ‘s’ shaped for *A. tricantha* and *A. excelsum*, and ‘r’ shaped for all other species (Fig. 1.1). Whereas liana species showed high (>-1.0 MPa) values for P_{50}, they also had very high values of $K_{S\ max}$ up to 27.8 kg m^{-1} s^{-1} MPa^{-1} such that most of these species still had a K_S above 5 kg m^{-1} s^{-1} MPa^{-1} as loss of hydraulic conductivity rose above 50% (Fig. 1.1). Tree species showed lower values of K_S at 50%

loss of conductivity and overall more gradual loss of hydraulic conductivity as water potential decreased compared to lianas (Fig. 1.1). We found evidence of a significant correlation and trade-off between water transport capacity and resistance to drought-induced xylem cavitation, as species with high $K_{S\ max}$ tended to exhibit less negative P_{50} (Fig. 1.2, Table 1.3). Values for $K_{S\ max}$ were also positively correlated with LA:SA (P = 0.02; Table 1.3), whereas $K_{L\ native}$ was negatively correlated with LA:SA only among tree species (r = –0.85, P = 0.03). P_{50} was negatively correlated with LA:SA (P = 0.03; Table 1.3) and P_e was negatively correlated with ρ_{wood} (P = 0.04; Table 1.3). Among tree species, P_e–P_{50} was negatively correlated with LA:SA (r = –0.93, P = 0.008).

There was a positive correlation between C and $\Psi_{leaf\ md}$ (Fig. 1.3, Table 1.3), indicating that high values for C buffer sapwood from reaching more negative values of Ψ_{leaf}. We found that C was significantly correlated with P_{50} within the tree growth form (r = 0.81, P = 0.05), but did not vary significantly with P_{50} within lianas or across all species (Table 1.3). Among lianas, C was negatively correlated with ρ_{wood} (r = –0.91, P = 0.01), but not among trees or across all species (Table 1.3).

We found evidence of coordination between leaf water status and stem traits. d_{branch} was positively correlated with $\Psi_{leaf\ md}$ (P = 0.02; Table 1.3) across species, and within lianas $\Psi_{leaf\ md}$ was positively correlated with ρ_{wood} (r = 0.88, P = 0.02) and SLA (r = –0.82, P = 0.05). We also found evidence of coordination between gas exchange and stem traits where $g_{s\ max}$ was positively correlated with P_e (P = 0.006; Table 1.3). Within the liana growth form, $g_{s\ max}$ was positively correlated with P_e–P_{50} (r = 0.88, P = 0.02).

Within lianas, $\delta^{13}C$ was positively correlated with ρ_{wood} ($r = 0.82$, $P = 0.05$) and $\Psi_{leaf\ md}$ ($r = 0.84$, $P = 0.04$), and negatively correlated with C ($r = -0.85$, $P = 0.03$).

Among leaf traits, N_{mass} was positively correlated with C ($P = 0.04$; Fig. 1.4a) across all species and with $K_{L\ max}$ within lianas ($P = 0.03$; Fig. 1.4b), but no relationship was found within trees because the point for *C. alliodora* failed the hat matrix procedure test for outliers. $\delta^{15}N$ was negatively correlated with $g_{s\ max}$ ($r = -0.75$, $P = 0.005$; Fig. 1.4c), and $\delta^{13}C$ was negatively correlated with SLA ($P = 0.02$; Fig 1.4d). N_{area} was also negatively correlated with SLA ($r = -0.64$, $P = 0.02$). Among lianas N_{area} was positively correlated with $\Psi_{leaf\ md}$ ($r = 0.90$, $P = 0.01$) and was negatively correlated with C ($r = -0.89$, $P = 0.01$).

All of the cross-species correlations, except the relationship between $\Psi_{leaf\ md}$ and C were also significant when evaluated as PICs (Table 1.3). We found more correlations in PICs than in cross-species correlations, especially those related to ρ_{wood}, P_{50} and d_{branch}, indicating that these correlations are the products of repeated evolutionary divergences in plant traits through evolutionary time, as well as being functionally correlated among extant species today. In addition to the significant relationship with $K_{S\ max}$, P_{50} was also related to $K_{L\ max}$ and P_e in PICs (Table 1.3). PIC analysis also showed significance in ρ_{wood}–$\Psi_{leaf\ md}$, d_{branch}–P_{50} and d_{branch}–$\Psi_{leaf\ md}$ relationships, which were not observed in cross-species analysis (Table 1.3).

The first PCA axis accounted for 29.70% of the variance (Fig. 1.5). The highest absolute eigenvector score for the negative range of the first PCA axis were the hydraulic safety margin P_e–P_{50}, $\Psi_{leaf\ md}$, and d_{branch}, whereas more vulnerable P_{50} values, $\Delta\Psi_{leaf}$, and

$K_{S\ max}$ loaded on the positive range of the first PCA axis. The second PCA axis accounted for 18.73% of the variance (Fig. 1.5). The highest absolute eigenvector score for the negative range of the second PCA axis were ρ_{wood} and P_e, whereas $K_{S\ native}$ and $g_{s\ max}$ loaded on the positive range of the second PCA axis.

Discussion

Our physiological measurements support the existence of a trade-off between efficiency, in the form of water transport capacity ($K_{S\ max}$) and safety, in the form resistance to drought-induced xylem cavitation (P_{50}) in trees and lianas. We found that trees exhibited greater resistance to water-stress-induced cavitation with more negative P_{50} values, higher capacitance, and a greater safety margin. In comparison lianas exhibited higher conductive capabilities than coexisting tree species, based on greater values of $K_{S\ max}$, $K_{L\ max}$, and $K_{S\ native}$. Our PCA analysis confirmed that trees and lianas separate along a principal axis determined by P_{50} and $K_{S\ max}$, among other variables. These results demonstrate that trees use more conservative strategies to maintain the soil-to-leaf hydraulic pathway than do lianas (Johnson *et al.*, 2013). Indeed our data demonstrate that most lianas exhibit higher absolute conductivity than trees even as they lose a higher percentage of conductive capability with declining water potential. The interspecific negative bivariate relationship between P_{50} and K_{Smax} agrees with previous findings of trade-offs between drought resistance and hydraulic transport (Pockman & Sperry, 2000; Maherali *et al.*, 2004; Gleason *et al.*, 2015), and illustrates how this relationship may structure a diverse assemblage of hydraulic strategies and competitive balance of trees and lianas in neotropical forest with regards to site water balance.

Plotting the reduction in K_S with declining water potential in vulnerability curves revealed patterns that are obscured by only examining percent loss of conductivity. Although lianas show a rapid decrease in K_S with declining water potential and P_{50} values ranging from -0.22 to -0.66 MPa, their high values of K_S max result in relatively high

values of K_S remaining even after losing more than 50% of hydraulic conductivity. For example, all liana species except *H. reclinata* showed K_S values above 5 kg m^{-1} s^{-1} MPa^{-1} after losing more than 50% of hydraulic conductivity, which is greater than 90% of the angiosperms investigated in the recent global meta-analysis of hydraulic safety versus efficiency (Gleason *et al.*, 2015). This pattern is likely due to heteroxyly in lianas, in which a wide variation in vessel sizes can be found in individual stems (Gentry, 1996; Rowe & Speck, 2005). The rapid decrease in hydraulic conductivity with declining water potential in lianas could represent the cavitation of a few of the largest vessels which might contribute disproportionately to high K_S, but might also be more vulnerable to cavitation by water stress. By contrast, trees showed a more gradual increase in percent loss of conductivity with declining water potential, resulting in a more conservative strategy than lianas. Our findings are consistent with previous studies at this site comparing lianas and trees. In comparing the tree species *A. excelsum* and two liana species, Johnson et al. (2013) also found lianas to be more vulnerable to cavitation. Yet, they reported similar values for K_S and ρ_{wood} between lianas and trees, which differs from our study because, when we added five other tree species and four other liana species to the comparison, we found that lianas had greater K_S and denser wood than trees.

Our findings that lianas had greater LA:SA than trees and that $K_{L\,max}$ was related to N_{mass} only for lianas suggest potential benefits in terms of photosynthetic productivity with high K_S in lianas in this seasonally dry forest. Both LA:SA and $K_{L\,max}$ are indices of water supply to leaves and the increase in N_{mass} with $K_{L\,max}$ in lianas supports the idea that plants are expected to allocate to relatively greater photosynthetic capacity as water

supply to leaves increases in order to take advantage of a high supply of CO_2 for photosynthesis (Santiago et al. 2004a). Greater K_L in lianas than in trees has been found in previous analyses comparing hydraulic capacity of lianas and trees (Patiño *et al.*, 1995; Santiago *et al.*, 2015), and is consistent with lianas as a hydraulically efficient growth form that occur on the fast-return side of the leaf economics spectrum (Wright et al. 2004; Maire et al. 2015). The extension of greater K_L to greater photosynthetic potential is also consistent with an analysis demonstrating greater concentrations of metabolically active elements in lianas and trees across 48 tropical forest sites (Asner & Martin, 2012). However, at high precipitation sites (>2500 mm rainfall yr^{-1}), lianas may lose their elevated leaf elemental concentration advantage to trees (Santiago & Wright, 2007; Asner & Martin, 2012). Further linkages between stem and leaf coordination of water loss and potential carbon gain were not evident in results of leaf $\delta^{13}C$ as there were no significant differences between lianas and trees. The only pattern in leaf $\delta^{13}C$ was a significant negative relationship with SLA indicating that thicker leaves incorporated more ^{13}C likely due to reduced CO_2 diffusion rates and low C_i in thick leaves (Vitousek *et al.*, 1990). Leaf $\delta^{15}N$ showed a significant negative relationship with $g_{s\,max}$ and significantly lower values in lianas than in trees, consistent with greater transpiration efficiency of N uptake in trees with lower rates of stomatal conductance (Cernusak et al. 2009).

Our study produced several striking results concerning biophysical properties of wood. First, lianas showed greater wood density than trees. We originally expected greater wood density in trees because of the well-known presence of large vessels in liana stems (Ewers & Fisher, 1991). However, it is critical to note that not only large vessels

characterize liana stems, but rather heteroxyly, the presence of a broad distribution of vessel sizes (Rowe & Speck, 2005). Furthermore, wood density is determined by the sum of vessels, fibres, and parenchyma cells, not only vessel size. The high number of vessels packed in liana stems, which is possible due to less investments in fibers for mechanical support, may determine the high wood density in lianas (Ewers *et al.*, 2015). Indeed, high vessel density has been shown to increase wood density (Martínez-Cabrera *et al.*, 2011). Our data is also consistent with at least one study from Parque Natural Metropolitano which reported dense wood in lianas (Johnson *et al.*, 2013), and also consistent with a previous finding that high wood density results in greater fluctuations in leaf water potential (Meinzer, 2003). Therefore, although wood density as a functional trait is generally related to growth and water transport capacity (Santiago et al. 2004a, Poorter et al. 2008), actual measures of stem anatomy are likely to determine the physiological roles of wood density and vessel size in hydraulic architecture.

The second striking result from our study illustrates that C is greater in trees than in lianas, is related to $\Psi_{\text{leaf md}}$ and is also related to N_{mass}. Thus, C appears to buffer leaves from rapid drops in water potential during high rates of transpiration. Additionally, C plays an important role in supplying water in species with a deciduous leafing habit (Wolfe & Kursar, 2015) and might also provide a physical space for a large reservoir of N needed for rapidly developing new leaves, and thus requires further investigation in seasonally dry tropical forests where many species, particularly trees, tend to be drought deciduous. Significantly lower LA:SA in trees also appears to promote a strong buffering effect on $\Psi_{\text{leaf md}}$. Finally, trees have greater terminal canopy stem diameters, a common

denominator that is positively correlated with predawn and midday water potential and negatively with P_{50}, and generally reduces shifts in leaf water potential and augments time lags of trees due to stem water storage (Goldstein *et al.*, 1998; Phillips *et al.*, 1999). In terms of increasing liana relative abundance in neotropical forests, our study represents the first comprehensive analysis of hydraulic safety and efficiency of a group of naturally established mature canopy tree and liana species. Our finding that lianas exhibit greater water transport capacity at the expense of vulnerability to drought-induced xylem cavitation suggests that hydraulic physiology could be a mechanism contributing to changes in relative abundance of lianas and trees in neotropical forests, especially if changes in temperature and precipitation patterns produce substantial alterations of water balance. Several studies document increases in liana density that coincide with long-term reductions in precipitation (Wright *et al.*, 2004a; Wright & Calderón, 2006; Ingwell *et al.*, 2010; Schnitzer *et al.*, 2012), yet a new long-term study shows increased liana relative abundance in undisturbed Amazonian forest with no significant change in local precipitation (Laurance *et al.*, 2014). Thus, whether it is changes in temperature, evaporative demand, precipitation, or other factors that are driving liana increases in the neotropics, the greater water transport capacity in lianas than in trees, along with greater potential belowground resource acquisition in lianas (Chen *et al.*, 2015; Collins *et al.*, 2016), represent mechanisms that could promote liana increases relative to trees. Yet, if climate change continues unabated, we are likely to see the development of tropical environments not previously observed in Earth's history (Chambers *et al.*, 2013), with habitats receiving greater than 3000 mm of precipitation with mean annual temperatures

> 30 °C. As temperatures and evaporative demand increase, greater vulnerability to drought-induced cavitation in lianas might become detrimental to their growth and survival, which could shift the competitive advantage back to trees. Overall, it appears that the hydraulic safety versus efficiency trade-off may shape differences in hydraulic function between lianas and trees with major implications for their relative abundance during climate change.

References

Ackerly DD. **2004**. Functional strategies of chaparral schrubs in relation to seasonal water deficit and distrubance. *Ecological Monographs* **74**: 25–44.

Alder N, Pockman WT, Sperry JS, Nuismer S. **1997**. Use of centrifugal force in the study of xylem cavitation. *Journal of Experimental Botany* **48**: 665–674.

Asner GP, Martin RE. **2012**. Contrasting leaf chemical traits in tropical lianas and trees: implications for future forest composition. *Ecology Letters* **15**: 1001–7.

Bucci SJ, Scholz FG, Goldstein G, Meinzer FC, Arce ME. **2009**. Soil water availability and rooting depth as determinants of hydraulic architecture of Patagonian woody species. *Oecologia* **160**: 631–641.

Chambers J, Negron Juarez R, Holm J, Knox R, Jardine K, McDowell NG, Di Vittorio A, Koven C, Higuchi N. **2013**. Tropical forests and the Earth system under a warming climate. *Eos Trans AGU, Fall Meet. Suppl., Abstract:* **B22C–07**.

Chave J, Olivier J, Bongers F, Châtelet P, Forget P-M, van der Meer P, Norden N, Riéra B, Charles-Dominique P. **2008**. Above-ground biomass and productivity in a rain forest of eastern South America. *Journal of Tropical Ecology* **24**: 355–366.

Choat B, Jansen S, Brodribb TJ, Cochard H, Delzon S, Bhaskar R, Bucci SJ, Feild TS, Gleason SM, Hacke UG, *et al*. **2012**. Global convergence in the vulnerability of forests to drought. *Nature* **491**: 752–5.

Collins CG, Wright SJ, Wurzburger N. **2016**. Root and leaf traits reflect distinct resource acquisition strategies in tropical lianas and trees. *Oecologia* **180**: 1037–1047.

Drake PL, Franks PJ. **2003**. Water resource partitioning, stem xylem hydraulic properties, and plant water use strategies in a seasonally dry riparian tropical rainforest. *Oecologia* **137**: 321–329.

Ewers FW, Fisher JB. **1991**. Why vines have narrow stems: Histological trends in Bauhinia (Fabaceae). *Oecologia* **88**: 233–237.

Feild TS, Balun L. **2008**. Xylem hydraulic and photosynthetic function of Gnetum (Gnetales) species from Papua New Guinea. *New Phytologist* **177**: 665–675.

Fortunel C, Ruelle J, Beauchêne J, Fine PVA, Baraloto C. **2014**. Wood specific gravity and anatomy of branches and roots in 113 Amazonian rainforest tree species across environmental gradients. *New Phytologist* **202**: 79–94.

Gartner BL, Bullock SH, Mooney HA, Brown VB, Whitbeck JL. **1990**. Water transport properties of vine and tree stems in a tropical deciduous forest. *American Journal of Botany* **77**: 742–749.

Gentry AH. **1996**. A field guide to the families and genera of woody plants of northwest South America (Columbia, Ecuador, Peru) with supplementary notes on herbaceous taxa. Chicago: University of Chicago Press.

Gerwing JJ, Farias DL. **2000**. Integrating liana abundance and forest stature into an estimate of total aboveground biomass for an eastern Amazonian forest. *Journal of Tropical Ecology* **16**: 327–335.

Gleason SM, Westoby M, Jansen S, Choat B, Hacke UG, Pratt RB, Bhaskar R, Brodribb TJ, Bucci SJ, Cao K, *et al*. 2015. Weak tradeoff between xylem safety and xylem-specific hydraulic efficiency across the world s woody plant species. New *Phytologist* **209**: 123–136.

Goldstein G, Andrade JL, Meinzer FC, Holbrook NM, Cavelier J, Jackson P. **1998**. Stem water storage and diurnal patterns of water use in tropical forest canopy trees. *Plant, Cell and Environment* **21**: 397–406.

Hacke UG, Sperry JS, Feild TS, Sano Y, Sikkema EH, Pittermann J. **2007**. Water Transport in Vesselless Angiosperms: Conducting Efficiency and Cavitation Safety. *International Journal of Plant Sciences* **168**: 1113–1126.

Hacke UG, Sperry JS, Wheeler JK, Castro L. **2006**. Scaling of angiosperm xylem structure with safety and efficiency. *Tree Physiology* **26**: 689–701.

Hacke UG, Venturas MD, MacKinnon ED, Jacobsen AL, Sperry JS, Pratt RB. **2015**. The standard centrifuge method accurately measures vulnerability curves of long-vesselled olive stems. *New Phytologist* **205**: 116–127.

Hammer Ø, Harper D, Ryan P. 2001. PAST: Paleontological Statistics Software Package for Education and Data Analysis. *Paleontologia Electronica*: 1–31.

Harrell Jr FE, Dupont C, *et al*. 2014. Hmisc: Harrel Miscellaneous.

Ingwell LL, Joseph Wright S, Becklund KK, Hubbell SP, Schnitzer SA. **2010**. The impact of lianas on 10 years of tree growth and mortality on Barro Colorado Island, Panama. *Journal of Ecology* **98**: 879–887.

Jacobsen AL, Ewers FW, Pratt RB. **2005**. Do xylem fibers affect vessel cavitation resistance? *Plant Physiology* **139**: 546–556.

Jacobsen AL, Pratt RB. **2012**. No evidence for an open vessel effect in centrifuge-based vulnerability curves of a long-vesselled liana (*Vitis vinifera*). *New Phytologist* **194**: 982–90.

Johnson DM, Domec J, Woodruff DR, McCulloh KA, Meinzer FC. **2013**. Contrasting hydraulic strategies in two tropical lianas and their host trees. *American Journal of Botany* **100**: 374–83.

Laurance WF, Andrade AS, Magrach A, Camargo JLC, Valsko JJ, Campbell M, Fearnside PM, Edwards W, Lovejoy TE, Laurance SG. **2014**. Long-term changes in liana abundance and forest dynamics in undisturbed Amazonian forests. *Ecology* **95**: 1604–1611.

Maherali H, Pockman WT, Jackson RB. **2004**. Adaptive variation in the vulnerability of woody plants to xylem cavitation. *Ecology* **85**: 2184–2199.

Martínez-Vilalta J, Piñol J, Beven K. **2002**. A hydraulic model to predict drought-induced mortality in woody plants: An application to climate change in the Mediterranean. *Ecological Modelling* **155**: 127–147.

Meinzer F. **2003**. Functional convergence in plant responses to the environment. *Oecologia* **134**: 1–11.

Meinzer FC, James SA, Goldstein G, Woodruff D. **2003**. Whole-tree water transport scales with sapwood capacitance in tropical forest canopy trees. *Plant, Cell and Environment* **26**: 1147–1155.

Meinzer FC, Johnson DM, Lachenbruch B, McCulloh KA, Woodruff DR. **2009**. Xylem hydraulic safety margins in woody plants: Coordination of stomatal control of xylem tension with hydraulic capacitance. *Functional Ecology* **23**: 922–930.

Patiño S, Tyree MT, Herre EA. **1995**. Comparison of hydraulic architecture of woody plants of differing phylogeny and growth form with special reference to free-standing and hemi-epiphytic Ficus species from Panama. *New Phytologist* **129**: 125–134.

Phillips OL, Vásquez Martínez R, Arroyo L, Baker TR, Killeen T, Lewis SL, Malhi Y, Monteagudo Mendoza A, Neill D, Núñez Vargas P, *et al*. 2002. Increasing dominance of large lianas in Amazonian forests. *Nature* **418**: 770–774.

Pockman WT, Sperry JS. **2000**. Vulnerability to xylem cavitation and the distribution of sonoran desert vegetation. *American Journal of Botany* **87**: 1287–1299.

Poorter L, Wright SJ, Paz H, Ackerly DD, Condit R, Ibarra-Manríquez G, Harms KE, Licona JC, Martínez-Ramos M, Mazer SJ, *et al*. 2008. Are functional traits good

predictors of demographic rates? Evidence from five neotropical forests. *Ecology* **89**: 1908–1920.

Pratt RB, Jacobsen AL, Ewers FW, Davis SD. **2007**. Relationships among xylem transport, biomechanics and storage in stems and roots of nine Rhamnaceae species of the California chaparral. *New Phytologist* **174**: 787–98.

Putz F. **1993**. Liana biomass and leaf-area of a 'Tierra Firme' forest in the Rio-Negro basin, Venezuela . *Biotropica* **15**: 185–189.

R Core Team. **2016**. R: A language and environment for statistical computing.

Restom TG, Nepstad DC. **2001**. Contribution of vines to the evapotranspiration of a secondary forest in eastern Amazonia. *Plant and Soil* **236**: 155–163.

Rowe N, Speck T. **2005**. Plant growth forms: an ecological and evolutionary perspective. *New Phytologist* **166**: 61–72.

van der Sande MT, Poorter L, Schnitzer SA, Markesteijn L. **2013**. Are lianas more drought-tolerant than trees? A test for the role of hydraulic architecture and other stem and leaf traits. *Oecologia* **172**: 961–72.

Santiago LS, Goldstein G, Meinzer FC, Fisher JB, Machado K, Woodruff D, Jones T. **2004a**. Leaf photosynthetic traits scale with hydraulic conductivity and wood density in Panamanian forest canopy trees. *Oecologia* **140**: 543–550.

Santiago LS, Kitajima K, Wright SJ, Mulkey SS. **2004b**. Coordinated changes in photosynthesis, water relations and leaf nutritional traits of canopy trees along a precipitation gradient in lowland tropical forest. *Oecologia* **139**: 495–502.

Santiago LS, Pasquini SC, De Guzman ME. **2015**. Physiologyical implications of the liana growth form. In: Schnitzer SA,, In: Bongers F,, In: Burnham R,, In: Putz FE, eds. Ecology of Lianas. Oxford: Wiley-Blackwell, 288–298.

Santiago LS, Wright SJ. **2007**. Leaf functional traits of tropical forest plants in relation to growth form. *Functional Ecology* **21**: 19–27.

Schnitzer SA. **2005**. A mechanistic explanation for global patterns of liana abundance and distribution. *The American Naturalist* **166**: 262–276.

Schnitzer SA, Bongers F. **2011**. Increasing liana abundance and biomass in tropical forests: emerging patterns and putative mechanisms. *Ecology Letters* **14**: 397–406.

Schnitzer SA, Bongers F, Burnham R, Putz FE. **2015**. Ecology of Lianas. Oxford: Wiley-Blackwell.

Schnitzer SA, Mangan SA, Dalling JW, Baldeck CA, Hubbell SP, Ledo A, Muller-Landau H, Tobin MF, Aguilar S, Brassfield D, *et al*. **2012**. Liana abundance, diversity, and distribution on Barro Colorado Island, Panama. *PloS ONE* **7**: e52114.

Sperry JS, Christman MA, Torres-Ruiz JM, Taneda H, Smith DD. **2012**. Vulnerability curves by centrifugation: is there an open vessel artefact, and are 'r' shaped curves necessarily invalid? *Plant, Cell and Environment* **35**: 601–10.

Sperry JS, Donnelly JR, Tyree MT. **1988**. A method for measuring hydraulic conductivity and embolism in xylem. *Plant, Cell and Environment* **11**: 35–40.

Sperry JS, Meinzer FC, McCulloh KA. **2008**. Safety and efficiency conflicts in hydraulic architecture: scaling from tissues to trees. *Plant, Cell and Environment* **31**: 632–645.

Tobin MF, Pratt RB, Jacobsen AL, De Guzman ME. **2013**. Xylem vulnerability to cavitation can be accurately characterised in species with long vessels using a centrifuge method. *Plant Biology* **15**: 496–504.

Torres-Ruiz JM, Sperry JS, Fernández JE. **2012**. Improving xylem hydraulic conductivity measurements by correcting the error caused by passive water uptake. *Physiologia Plantarum* **146**: 129–35.

Tyree MT, Davis SD, Cochard H. **1994**. Biophysical perspectives of xylem evolution: is there a tradeoff of hydraulic efficiency for vulnerability to dysfunction? *IAWA Journal* **15**: 335–360.

Webb CO, Ackerly DD, Kembel S. **2009**. Phylocom: software for the analysis of phylogenetic community structure and character evolution (with phylomatic and ecovolve)-user's manual version 4.1.

Wheeler JK, Sperry JS, Hacke UG, Hoang N. **2005**. Inter-vessel pitting and cavitation in woody Rosaceae and other vesselled plants: A basis for a safety versus efficiency trade-off in xylem transport. *Plant, Cell and Environment* **28**: 800–812.

Wolfe BT, Kursar TA. **2015**. Diverse patterns of stored water use among saplings in seasonally dry tropical forests. *Oecologia* **179**: 925–936.

Wright SJ, Calderón O. **2006**. Seasonal, El Niño and longer term changes in flower and seed production in a moist tropical forest. *Ecology Letters* **9**: 35–44.

Wright SJ, Calderon O, Hernandez A, Paton S. **2004**. Are lianas increasing in importance in tropical forests? A 17-year record from Panama. *Ecology* **85**: 484–489.

Zhu S-D, Cao K-F. **2009**. Hydraulic properties and photosynthetic rates in co-occurring lianas and trees in a seasonal tropical rainforest in southwestern China. *Plant Ecology* **204**: 295–304.

Zhu S-D, Cao K-F. **2010**. Contrasting cost-benefit strategy between lianas and trees in a tropical seasonal rain forest in southwestern China. *Oecologia* **163**: 591–9.

Figures and Tables

Table 1.1. Plant species, growth form classification, family, symbol and phenology from Parque Metropolitano Natural. Phenology is based on Croat (1978).

Species	Family	Symbol	Phenology
Tree species:			
Anacardium excelsum (Bertero & Balb. ex Kunth) Skeels	Anacardiaceae	▲	Evergreen
Annona spraguei Saff.	Annonaceae	●	Semi-deciduous
Antirrhoea trichantha Hemsl.	Rubiaceae	■	Deciduous
Astronium graveolens Jacq.	Anacardiaceae	◆	Semi-deciduous
Cordia alliodora (Ruiz & Pav.) Cham. ex A. DC.	Boraginaceae	⬢	Deciduous
Luehea seemannii Triana & Planch.	Malvaceae	★	Evergreen
Liana species:			
Arrabidaea patellifera (Schltdl.) Sandwith	Bignoniaceae	△	Evergreen
Combretum fruticosum (Loefl.) Fawc. & Rendle	Combretaceae	○	Deciduous
Doliocarpus dentatus (Aubl.) Standl.	Dilleniaceae	□	Evergreen
Hiraea reclinata Jacq.	Malpighiaceae	◇	Evergreen
Mikania leiostachya Benth.	Asteraceae	⬡	Evergreen
Serjania mexicana L. (Wild.)	Sapindaceae	☆	Evergreen

Table 1.2. Summary of traits for tree and liana growth forms. The values are reported as mean ± SE. Test statistic reported are from either student's *t*-test or Mann-Whitney *U* test.

Variable	Tree	Liana	Test statistic	p-value
P_{50} (MPa)	-0.70 ± 0.08	-0.35 ± 0.04	4.06	<0.001
C (kg m^{-3} MPa^{-1})	453 ± 41	273 ± 23	-3.83	<0.001
$K_{S\ max}$ (kg m^{-1} s^{-1} MPa^{-1})	5.31 ± 0.73	10.50 ± 1.75	2.87	0.007
$K_{L\ max}$ (kg m^{-1} s^{-1} MPa^{-1})	0.60 x 10^{-3} ± 0.09 x 10^{-3}	0.99 x 10^{-3} ± 0.15 x 10^{-3}	2.27	0.026
$K_{S\ native}$ (kg m^{-1} s^{-1} MPa^{-1})	1.63 ± 0.29	3.82 ± 0.75	2.73	0.009
$K_{L\ native}$ (kg m^{-1} s^{-1} MPa^{-1})	0.23 x 10^{-3} ± 0.05 x 10^{-3}	0.39 x 10^{-3} ± 0.08 x 10^{-3}	1.78	0.079
$\Delta\Psi_{leaf}$ (MPa)	0.69 ± 0.10	0.98 ± 0.08	2.38	0.023
$\Psi_{leaf\ pd}$ (MPa)	-0.30 ± 0.03	-0.33 ± 0.03	145	0.591
$\Psi_{leaf\ md}$ (MPa)	-0.99 ± 0.09	-1.31 ± 0.08	-2.72	0.010
$\Psi_{stem\ native}$ (MPa)	-0.62 ± 0.06	-0.81 ± 0.07	-2.06	0.043
P_e (MPa)	59 x 10^{-3} ± 17 x 10^{-3}	56 x 10^{-3} ± 19 x 10^{-3}	652	0.696
$P_e - P_{50}$ (MPa)	0.72 ± 0.07	0.39 ± 0.04	304	<0.001
$g_{s\ max}$ (mmol m^{-2} s^{-1})	169 ± 15	193 ± 19	0.978	0.335
ρ_{wood} (g cm^{-3})	0.34 ± 0.01	0.43 ± 0.03	2.74	0.009
LA:SA (m^2 m^{-2})	8323 ± 611	14498 ± 1987	720	0.042
SLA (cm^2 g^{-1})	138 ± 8.8	148 ± 7.8	-0.697	0.489
d_{branch} (mm)	8.58 ± 0.33	5.75 ± 0.15	-7.79	<0.001
$\delta^{15}N$ (‰)	1.35 ± 0.20	0.79 ± 0.21	-1.90	0.061
$\delta^{13}C$ (‰)	-29.9 ± 0.23	-30.3 ± 0.21	-1.08	0.283
N_{mass} (mg g^{-1})	23.5 ± 1.15	21.3 ± 0.72	503	0.202
N_{area} (g cm^{-2})	0.18 ± 0.009	0.16 ± 0.009	-2.08	0.042

Abbreviations: Capacitance (C), water potential at 50% loss in hydraulic conductivity (P_{50}), maximum sapwood specific hydraulic conductivity ($K_{S\ max}$), maximum leaf specific hydraulic conductivity ($K_{L\ max}$), native sapwood specific hydraulic conductivity ($K_{S\ native}$), and native leaf specific hydraulic conductivity ($K_{L\ native}$). Diurnal change in leaf water potential ($\Delta\Psi_{leaf}$), predawn leaf water potential ($\Psi_{leaf\ pd}$), midday leaf water potential ($\Psi_{leaf\ md}$), native stem water potential ($\Psi_{stem\ native}$), air entry threshold (P_e), steepness of vulnerability curve ($P_e - P_{50}$), maximum stomatal conductance ($g_{s\ max}$), sapwood density (ρ_{wood}), leaf area to sapwood area ratio (LA:SA), specific leaf area (SLA), stem diameter (d_{branch}), nitrogen isotopic composition ($\delta^{15}N$), carbon isotopic composition ($\delta^{13}C$), nitrogen per leaf mass (N_{mass}), and nitrogen per leaf area (N_{area}).

Table 1.3. Pearson product-moment correlation coefficients (r) for species traits are given in the upper right section of the matrix (n = 12). Correlation coefficients for independent contrasts are given in the lower left section of the matrix (n = 12). Bold type indicates significant correlations ($P \leq 0.05$). Wood density (ρ_{wood}; g cm^{-3}), capacitance (C; kg m^{-3} MPa^{-1}), water potential at 50% loss in hydraulic conductivity (P_{50}; MPa), maximum xylem specific hydraulic conductivity ($K_{S\ max}$; kg m^{-1} s^{-1} MPa^{-1}), maximum leaf specific hydraulic conductivity ($K_{L\ max}$; kg m^{-1} s^{-1} MPa^{-1}), air entry threshold (P_e), predawn leaf water potential ($\Psi_{leaf\ pd}$; MPa), midday leaf water potential ($\Psi_{leaf\ md}$; MPa), maximum stomatal conductance ($g_{s\ max}$; mmol m^{-2} s^{-1}), leaf area to sapwood area ratio (LA:SA, m^2 m^{-2}), and branch diameter (d_{branch}, mm).

	ρ_{wood}	C	P_{50}	$K_{S\ max}$	$K_{L\ max}$	P_e	$\Psi_{leaf\ pd}$	$\Psi_{leaf\ md}$	$g_{s\ max}$	LA:SA	d_{branch}
ρ_{wood}		-0.508	-0.068	-0.216	0.053	**-0.600**	-0.386	-0.534	-0.250	-0.201	-0.279
C	-0.496		0.209	-0.011	-0.003	0.443	-0.039	**0.590**	-0.066	-0.045	0.242
P_{50}	-0.041	0.260		**0.650**	0.512	0.534	-0.111	-0.238	0.305	**0.630**	-0.540
$K_{S\ max}$	-0.061	-0.142	**0.727**		0.800	0.403	0.186	-0.268	0.232	**0.653**	-0.243
$K_{L\ max}$	0.271	-0.008	**0.718**	0.841		0.349	0.106	-0.432	0.327	0.207	-0.329
P_e	**-0.597**	0.382	**0.620**	0.442	0.433		-0.079	0.334	**0.744**	0.292	-0.063
$\Psi_{leaf\ pd}$	-0.410	-0.147	-0.564	0.270	0.390	-0.184		-0.064	-0.110	-0.037	0.279
$\Psi_{leaf\ md}$	**-0.601**	0.494	-0.301	-0.375	-0.553	0.273	-0.278		0.073	-0.225	**0.661**
$g_{s\ max}$	-0.309	-0.260	0.337	0.335	0.368	**0.790**	-0.197	0.127		0.155	-0.291
LA:SA	-0.217	-0.173	**0.605**	**0.813**	0.361	0.333	-0.475	-0.332	0.141		-0.426
d_{branch}	-0.225	0.090	**-0.625**	-0.354	-0.424	-0.181	**0.633**	**0.619**	-0.237	-0.555	

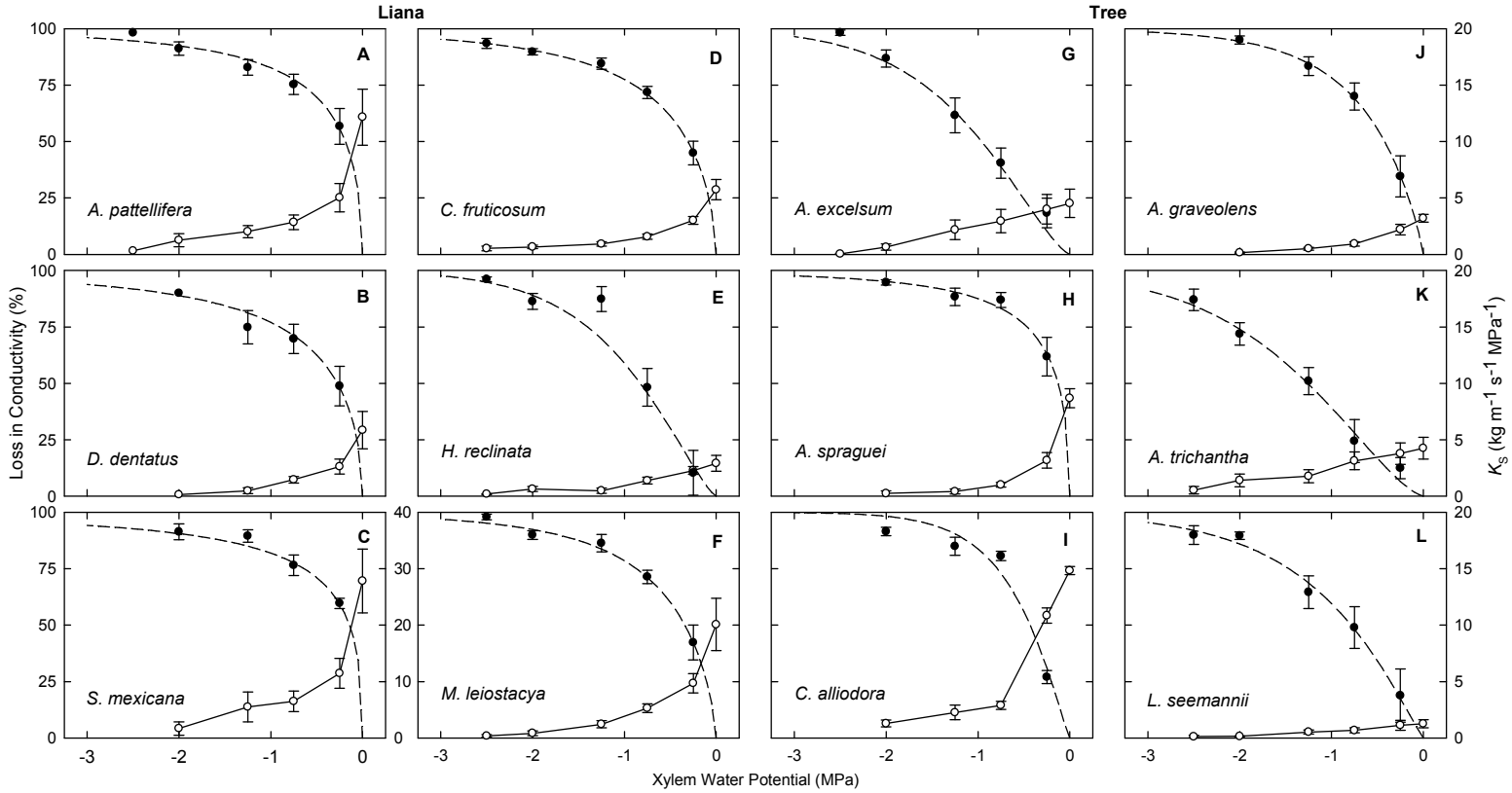

Figure 1.1. Xylem vulnerability to cavitation curves of lianas (A-F) and trees (G-L) during the wet season (June – August 2012; mean ± SE; $n = 6$, except for *C. alliodora* with $n = 3$) expressed as percent loss in conductivity (PLC, closed circle symbol and broken line) and expressed as hydraulic conductivity values (K_S, open circle symbol and solid line). Only *S. mexicana* (C) have a different K_S scale, which is indicated to the right of the plot.

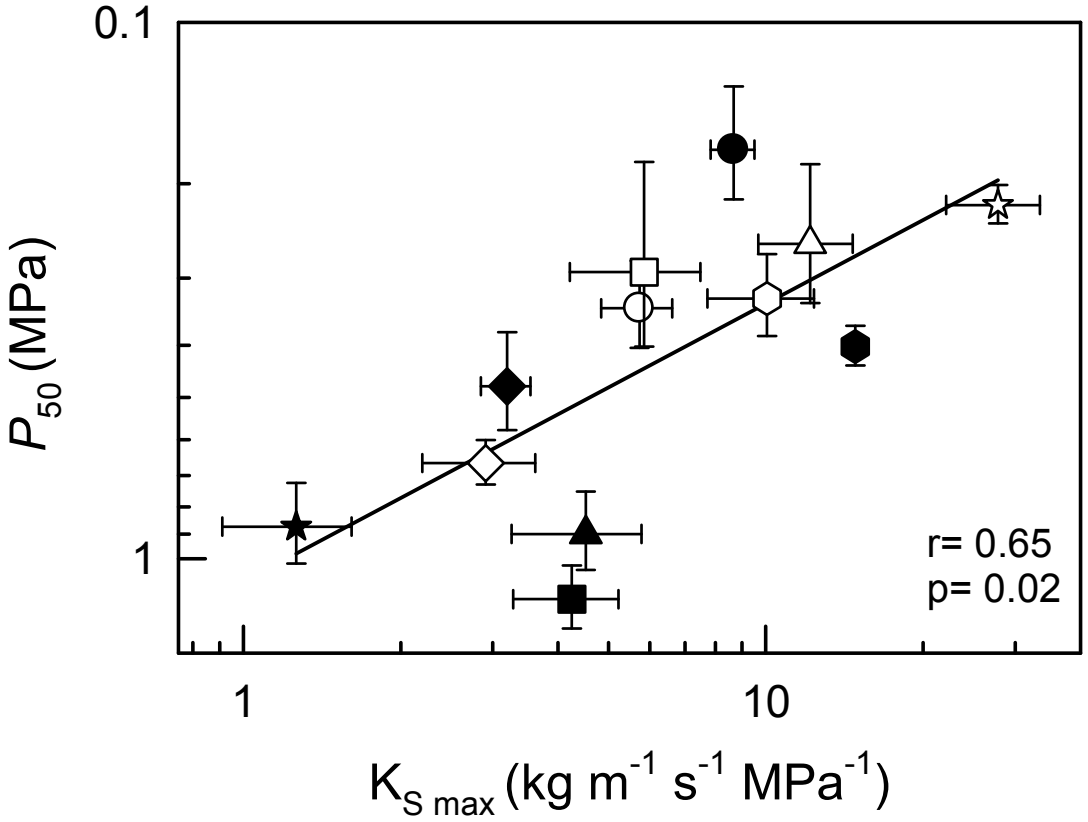

Figure 1.2. Relationship between maximum sapwood-specific conductivity and pressure causing 50% loss in hydraulic conductivity. Each symbol represents the mean ± SE for each species (n = 6, n = 3 for *C. alliodora*). Corresponding species and symbols are found in Table 1. Close symbols represent tree species and open symbols represent liana species.

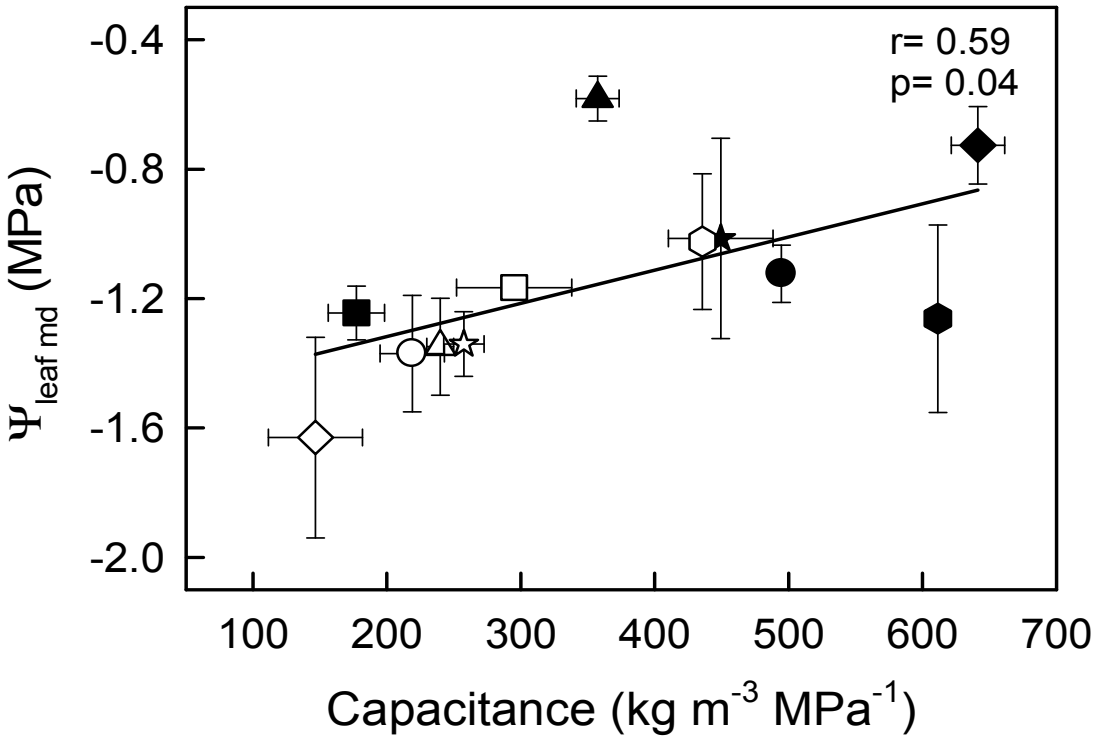

Figure 1.3. Relationship between capacitance and midday leaf water potential. Each symbol represents the mean ± SE for each species (n = 3). Corresponding species and symbols can be found in Table 1. Close symbols represent tree species and open symbols represent liana species.

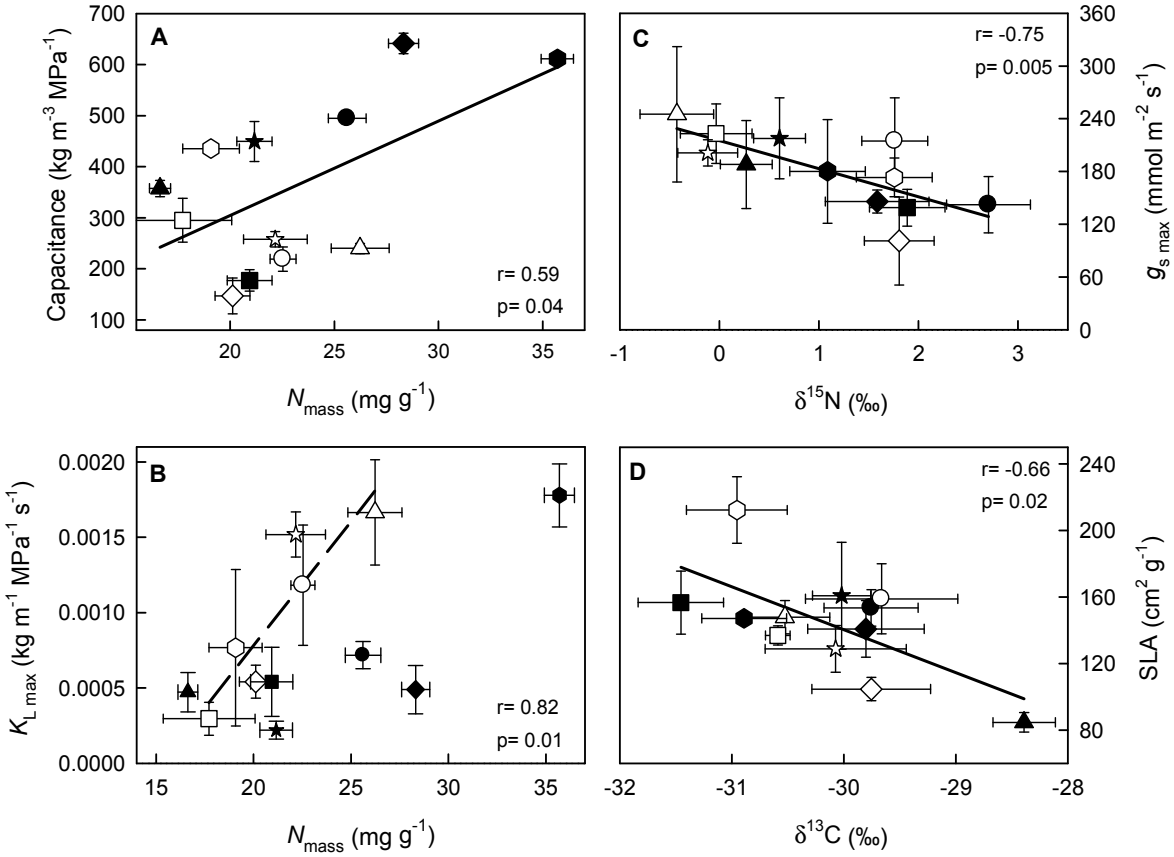

Figure 1.4. The relationship between leaf nitrogen per mass (N_{mass}) and **A** capacitance and **B** maximum leaf specific hydraulic conductivity ($K_{L\,max}$); between **C** leaf N isotopic composition ($\delta^{15}N$) and maximum stomatal conductance ($g_{s\,max}$); and between **D** leaf C isotopic composition ($\delta^{13}C$) and leaf specific leaf area (SLA). No relationship occurred for trees between N_{mass} and **B** $K_{L\,max}$ due to failing the outlier test. Corresponding species and symbols are found in Table 1. Close symbols represent tree species and open symbols represent liana species. Each symbol represents the mean ± SE for each species (n = 6, n = 3 for *C. alliodora*). Solid line represent correlations that include both trees and lianas while broken line represent correlation for lianas only.

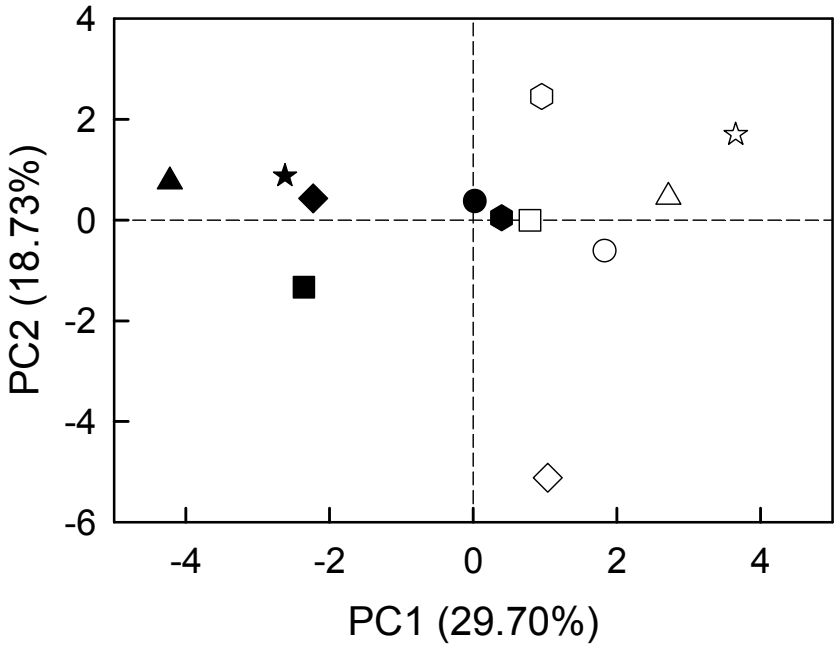

Figure 1.5. Principal components analysis ordination for tree species (closed symbols) and liana species (open symbols) based on 21 traits measured. The percentages in the axis labels indicate the variance explained by the axis. Corresponding species and symbols are found in Table 1.

Chapter 2

Coordination between maximization of sap transport and drought avoidance traits in canopy stems: evidence of hydraulic segmentation through vessel occlusion formation in lowland Amazonian forest.

Abstract

Maintaining the integrity of hydraulic transport in trees is crucial to leaf physiological function. Plants are able to maintain water supply to leaves by modifying different aspects of hydraulic transport, such as stem hydraulic conductance, resistance, and capacitance. We compared the hydraulic physiology of canopy branches in a lowland tropical Amazonian forest to examine the relationships among hydraulic conductivity, hydraulic segmentation, and xylem capacitance. We found that hydraulic segmentation and vulnerability segmentation traits were correlated, such that higher levels of vessel occlusion resulted in greater Ψ_{leaf}-Ψ_{stem} disequilibrium. Furthermore, we found that both aforementioned traits were associated with greater hydraulic conductance and greater capacitance at the expense of being more vulnerable to drought induced cavitation. This suggests that plants were able to maximize water transport by incorporating traits that modulated the hydraulic transport system within the xylem during times when water availability was limiting.

Introduction

Gas exchange in leaves occurs at the expense of substantial water loss during photosynthesis. A continuous column of water is supplied through xylem extending from the site of evaporation in the leaves through the stem and into the roots that are in contact with water in the soil, and this pathway is known as the soil-plant-atmosphere-continuum (SPAC). The process of water transport through the SPAC is described by the cohesion-tension theory which posits that intermolecular forces create a continuous column of water via 'cohesion' among water molecules and adhesion to xylem vessel walls, and that the evaporation of water on the leaves generates the 'tension' (negative water potential) that creates the driving force to transport water against gravity (Dixon & Joly, 1895). The constant struggle of plants in the environment to both safely and efficiently transport water through SPAC has resulted in the manifestation of diverse xylem forms in extant plants (Tyree & Zimmermann, 2002), which consequently generate different transport strategies among plant species.

The resulting diverse hydraulic strategies among plant species are the culmination of coordinated changes in the hydraulic conductive properties of xylem, including resistance to cavitation and embolism formation in xylem vessels, ability to localize cavitation in expendable organs, and capacity to store water in the xylem tissue. Hydraulic conductivity describes the relationship between the flow rate of water and the driving pressure gradient as it passes through a length of xylem tissue (Sperry *et al.*, 1988). The flow rate is proportional to the fourth power of the radius of the conduits within the xylem tissue (Tyree & Zimmermann, 2002), and thus slight changes in the

radii result in a significant change in conductivity. Xylem resistance to cavitation describes its ability to resist air entry into the lumens of conducting vessels rendering them nonfunctional. Cavitation resistance could arise from changes in different xylem traits, such as changes in fiber tissues (Jacobsen *et al.*, 2005), pit membrane structure (Wheeler *et al.*, 2005), or vessel networks (Lens *et al.*, 2011). The hydraulic segmentation hypothesis describes the different distribution of hydraulic resistances among plant organs along SPAC where distal organs are predicted to exhibit the highest resistance to flow. The hydraulic segmentation hypothesis may be separated into two ideas, with hydraulic segmentation suggesting that cavitation should be confined to distal organs that contain less carbon investment relative to the main trunk (Zimmermann, 1983) or vulnerability segmentation which suggests that cavitation should be confined to expendable organs such as fine roots and leaves (Sperry, 1986; Tyree & Ewers, 1991). Sapwood capacitance describes the water-storage capacity in the plant that can be extracted per change in water potential and functions as a buffering mechanism through either capillary storage, elastic cell deformation, or cavitation release (Zimmermann, 1983; Holbrook, 1995; Meinzer *et al.*, 2003). Plants may employ different combination of the traits described above depending on evolutionary history and environmental conditions. Furthermore, some of these traits may be mutually exclusive and align along common axes and thus characterize trade-offs.

The trade-off between hydraulic conductivity and cavitation resistance is well characterized. The empirical data gathered for conductance-resistance relationships in the past four decades have culminated with the synthesis of the hydraulic safety-efficiency

trade-off as an axis of plant functional trait variation (Westoby & Wright, 2006). In plant hydraulic transport, the safety-efficiency trade-off describes the transport strategies utilized by plants with cavitation resistant xylem with low conductive capacity on one end of the spectrum and vulnerable xylem with high capacity for transport on the other end of the spectrum (Maherali *et al.*, 2004). A synthesis of data for the safety-efficiency trade-off showed that most plants operate within a narrow range of hydraulic transport efficiency relative to the risk of hydraulic failure, regardless of environment (Choat *et al.*, 2012). Furthermore, the same global dataset has also demonstrated other aspects of hydraulic transport. For example, a recent meta-analysis revealed a significant but weak trade-off between safety and efficiency, with most plants occurring in the vulnerable and inefficient region of the axis. This suggests there may be important traits that explain diverse plant strategies that are orthogonal to the safety-efficiency axis (Gleason *et al.*, 2015), thus, highlighting the importance of the hydraulic traits that describe processes outside the conductance-resistance analog, such as capacitance.

Similar to the safety-efficiency trade-off, research supports capacitance as an axis of hydraulic trait variation. Capacitance trades-off with wood density and cavitation resistance such that higher capacitive discharge is known to occur in plants with low wood density and highly vulnerable xylem (Borchert & Pockman, 2005; Pratt *et al.*, 2007; McCulloh *et al.*, 2014; Richards *et al.*, 2014), to buffer fluctuations in plant water status (Phillips *et al.*, 1999; Meinzer *et al.*, 2003, 2008, 2009; Vergeynst *et al.*, 2014; Gleason *et al.*, 2014; De Guzman *et al.*, 2016), and to function as water recharge (Phillips *et al.*, 1999; Scholz *et al.*, 2007; Oliva Carrasco *et al.*, 2014; Vergeynst *et al.*, 2014;

Wolfe & Kursar, 2015). Furthermore, capacitance mirrors the adjustments of wood density relative to precipitation in that higher levels of water availability modulate maximum capacitance (Naidoo *et al.*, 2006; Richards *et al.*, 2014).

Unlike conductance, cavitation-resistance, and capacitance traits, hydraulic segmentation traits have not been extensively examined within tropical forests. However, current evidence available from other systems supports the function of hydraulic segmentation to either create resistance in hydraulic conductivity or disconnect the water flow in the SPAC when transpiration becomes too hydraulically demanding (Hao *et al.*, 2008; Pivovaroff *et al.*, 2014; Nolf *et al.*, 2015). One of the reasons why hydraulic physiology traits have been under-studied in tropical forests is due to the combination of difficult research logistics and due to species-specific difficulties associated with measuring hydraulic conductivity, such as xylem blockage, that results in systematic exclusion of some species from studies.

Xylem blockages can induce changes in hydraulic conductance that are not immediately reversible. Blockages may be the result of cavitation in vessels and subsequent formation of emboli or they may be more permanent vessel occlusions that represent exudates (gums, gels, resins, etc.) or cellular growth (tyloses) that block vessel lumens (Zimmermann, 1983). Vessel blockages may also result from the growth of bacteria or fungus within the vessel. The first detailed accounts of vessel occlusion have been attributed to Hermine, Baroness von Reichenbach of Vienna who recognized that cavitation or wounding was a precursor to the onset of vessel occlusion (Zimmermann, 1979). Since then, more has been discovered about vessel occlusions (De Micco *et al.*,

2016) such as empirical evidence to support vessel occlusion occurrence after cavitation and during drought stress (Klein, 1923; Rickard & Marriott, 1979; Jacobsen & Pratt, 2012) and also evidence to support vessel occlusion formation in response to wounding (ethylene) or infection without the occurrence of cavitation (Sun *et al.*, 2007). There are also many different types of vessel occlusions (Chattaway, 1949; Sun *et al.*, 2008), and linking the occurrence of vessel occlusions to different angiosperm lineages and specific aspects of xylem structure (Chattaway, 1949; Bonsen & Kučera, 1990). The tight link between the occurrence of vessel occlusions with living parenchyma cells (De Micco *et al.*, 2016) presents an opportunity to investigate how vessel occlusions relate to other components in the xylem tissues such as vessel and fiber fractions, and also how vessel occlusion formation relates to the constitution of the xylem matrix, such as how many vessels can be packed in a limited space. We were interested in examining how the formation of vessel occlusions related to drought response strategies.

Plant drought response strategies have been placed in a continuum from avoidance to tolerance (Levitt, 1972), but are not mutually exclusive as a combination of both strategies could be utilized by the same plant (Chaves *et al.*, 2003). Drought avoidance is characterized by traits that promote continued plant functioning by preventing the SPAC from experiencing low levels of water potential by adjustments in the supply-demand components (Sperry and Love 2015). For example, the supply component of transpiring leaves could be increased by access to more water resources deeper in the soil (Wagner *et al.*, 2011; Stahl *et al.*, 2013) or by modulating the water holding capacity in organs upstream to the leaves via capacitance. Furthermore, the

demand components could be changed by either reducing the transpirational demand via tight stomatal control (Skelton *et al.*, 2015), hydraulic segmentation (Pivovaroff *et al.*, 2014), or by disconnecting the flow through the SPAC through vulnerability segmentation via leaves (Tyree *et al.*, 1993; Nolf *et al.*, 2015; Wolfe *et al.*, 2016). Drought tolerance is characterized by traits that promote continued plant functioning by mitigating the effects of lowering levels of water potential in the SPAC through investments in structure. For example, drought tolerance can be achieved through carbon investments in building cavitation resistant xylem vessels (Hacke *et al.*, 2001; Jacobsen *et al.*, 2005; Choat & Pittermann, 2009) and osmotic adjustments in leaves (Bartlett *et al.*, 2014; Maréchaux *et al.*, 2015). These are by no means an exhaustive list of drought strategies, and there are other drought survival traits that contribute to both drought tolerance and avoidance (Pivovaroff et al. 2016; Santiago et al. 2016). However, evaluating drought response strategies creates a framework where we can explore the degree to which occlusion formation can be effectively added as a drought survival trait.

Understanding how the coordination of hydraulic traits interacts with drought is of critical importance as it gives us a mechanistic view of the hydraulic strategies utilized by plants in face of limited water availability. In tropical systems, we have wealth of information on both wood functional traits and long-term demographic data across diverse plant lineages. However, hydraulic physiological data are currently underrepresented.

In this study, we examined hydraulic strategies by characterizing the hydraulic traits of trees stratified across wood density in the lowland tropical forest of eastern

Amazonia in French Guiana. Our goal was to quantify hydraulic traits, and particularly vessel occlusion formation, to directly assess how vessel occlusion formation is coordinated with other hydraulic traits. We hypothesized that the formation of vessel occlusions is a drought avoidance trait that reduces the maximum transport capacity of xylem as drought progresses and that it is coordinated with vulnerability segmentation trait. We examined vulnerability segmentation by characterizing the leaf and stem water potential as the dehydration progressed. Among drought strategy traits, we hypothesize a correlation between drought avoidance traits with transport and architecture. Furthermore, we hypothesized a trade-off between drought avoidance and drought tolerance traits. Finally, we combined our data with a database of anatomical traits to examine how hydraulic traits related to constitution of the xylem tissue.

Materials and Methods

Study site and species

The study was conducted in a lowland tropical forest at Paracou Research Station, French Guiana (5°18'N; 52°53'W). The site is a seasonally dry terra firme rain forest with a distinct wet season that occurs from December to July that is interrupted by a brief dry season in March, and a more substantial dry season between the months of August and November with September and October receiving the least amount of rainfall (< 30 mm/month). The site had an annual rainfall of 2.73 m and an average temperature of 25.6°C during the sampling year (2014). The soils in the site are shallow ferralitic soils, limited in depth by a more or less transformed loamy saprolite (Gourlet-Fleury *et al.*, 2004). Measurements were conducted on 14 species (Table 2.1) selected to stratify across wood density values. Sun exposed canopy branches were sampled with the aid of professional climbers during the months of September and October. Samples that were two to three meters in length were harvested from the upper canopies with a saw between 0800 and 1100 h. The cut end was immediately sealed with parafilm and packing tape and the whole sample was double bagged in opaque bags with moist paper towels and sealed for transport to the laboratory. Each species were sampled on at least two to three individual trees at different sample dates during the sampling period. One large branch was collected from each tree that were subsampled twice per day at decreasing water potentials.

Bench top dehydration and water potential determination

After allowing the bagged branch to equilibrate in an air conditioned room (~24°C) between 8 – 16 h, the sealed bags were cut longitudinally to allow the collection of subsamples for the determination of hydraulic conductivity (K_H) related measurements, the native water potential of the leaf distal to the stem (Ψ_{leaf}), the native water potential of the conductive stem (Ψ_{stem}), and determination of capacitance related measurements. The bag was allowed to remain open for 1 h to partially dehydrate the branch and was subsequently sealed using clips and moist cloths for re-equilibration. This process was repeated to generate the different levels of cavitation and also repeated until either a very low water potential was achieved or the branch ran out of subsamples.

Prior to cutting the stem, three leaves distal to the branch were collected for determination of Ψ_{leaf} equilibrated with the stem using a Scholander pressure chamber (model 1000; PMS Instruments, Corvalis, Oregon, USA). Subsamples were cut from the main branch underwater in a plastic tub. The samples to be used for K_H and C were cut under water while the distal branch with the leaves was kept to determine the distal leaf area. For each subsample, a wood segment approximately 3 mm thick and 6 mm wide was cut from the blotted proximal end of the distal branch and was placed in a thermocouple psychrometer chamber (C-52; Wescor, Logan, UT, USA) connected to a data logger (PSΨPRO; Wescor, Logan, UT, USA) to determine Ψ_{stem}.

To determine vulnerability segmentation (Ψ_D; MPa MPa^{-1}), Ψ_{leaf} was plotted against Ψ_{stem} (Fig. 2.4). A linear regression was fitted to the points and the slope was

determined as an estimate of water potential disequilibrium. High slope values indicate greater water potential disequilibrium between leaf and stem.

Hydraulic measurements

K_H was determined gravimetrically by perfusing the stem with filtered (0.2 μm) degassed 20 mM KCl solution. The perfusion liquid was set at an elevated pressure head (< 2 kPa), and allowed to flow through the stem into a graduated 1 ml pipette (KIMAX-51; Kimble Chase, Vineland, NJ, USA) to measure the volumetric rates of flow to determine conductivity (Sperry *et al.*, 1988). Native hydraulic conductivity (K_{native}) measurements were determined for each branchlet subsampled *ca.* 1 m distal to the cut end after each stage of equilibration. Maximum hydraulic conductivity (K_{max}) was measured by removing native emboli after each K_{native} by flushing the samples with filtered and degassed perfusion liquid using a captive airtank (100 kPa) for 1 h. The percent loss in conductivity (PLC) was determined by subtracting the ratio between K_{native} and K_{max} from 1 and multiplying by 100. For some species K_{max} was set as the absolute maximum during the first day of measurements due to the progressive decline in K_{max} as the samples dehydrated (Fig. 2.7). The PLC was plotted against Ψ_{stem} and Ψ_{leaf} (Fig. 2.5) and fitted with a 2-parameter cumulative distribution Weibull function using Microsoft Excel solver to determine the hydraulic characteristics of the stem (Meinzer *et al.*, 2009). The index for resistance to drought-induced xylem cavitation was determined as the water potential at 50 percent loss in conductivity as calculated using the Weibull fit calculated for each species (P_{50}; MPa). The water potential at which cavitation initiates in the stem (P_e; MPa) was determined by calculating the Ψ_{stem}–axis intercept of the line

tangent to P_{50}. The steepness of the rate of loss in conductivity ($P_e - P_{50}$; MPa) was estimated by subtracting P_{50} from P_e, where low values indicate the highest rate of cavitation in the stem.

Maximum hydraulic conductance was calculated as both the maximum sapwood specific conductivity ($K_{S\,max}$; kg m^{-1} s^{-1} MPa^{-1}) by dividing K_{max} with the cross sectional sapwood area and as the maximum leaf specific conductivity ($K_{L\,max}$; kg m^{-1} s^{-1} MPa^{-1}) by dividing K_{max} with leaf area distal to the stem. The cross sectional sapwood area was determined from measuring the sapwood area on both cut ends of the stem by subtracting the total pith area from the sapwood. The distal leaf area was estimated by multiplying the total number of leaves by the average area of 10 representative leaves. The ratio between transpiration demand in leaves and hydraulic supply in stem is a key component of the plant hydraulic architecture (Whitehead *et al.* 1984); the ratio was estimated by dividing the total distal leaf area by the sapwood area of the stem (*LA:SA*; m^2 m^{-2}). The inverse of the *LA:SA* is also known as the Huber value (Tyree & Zimmermann, 2002).

The degree of vessel occlusion formation (O; kg m^{-1} s^{-1} MPa^{-1} day^{-1}) was quantified by calculating the decline of $K_{S\,max}$ over the days of bench top dehydration (Fig. 2.6). The slope of the relationship between time dehydrated and $K_{S\,max}$ multiplied by negative one was used as an indicator to reflect the varying degrees of occlusion formation between species. With this index, greater values indicate high levels of occlusion formation impact on hydraulic function.

Capacitance and wood density

Terminal stem samples 5-10 mm in diameter and 3-5 cm in length were collected from each sample branch upon arrival to the laboratory and were placed under degassed filtered water under light vacuum for rehydration overnight. We cut the sample to 10 mm in length, removed bark and pith to isolate xylem while submerged under filtered water, recorded volume, blotted to record saturated mass, and subsequently sealed them in psychrometer chambers. Xylem water potential (Ψ_x) was measured with a thermocouple psychrometer (75-3VC Small Chamber Thermocouple Psychrometer; Merrill Instruments, Logan, UT, USA) connected to a water potential datalogger (PSYPRO, Wescor Inc.) and placed inside an insulated chamber at 24°C. Values were logged every 0.5 h and Ψ_x was recorded when stable readings were achieved, alternated with measurements of fresh mass until a Ψ_x of -6 MPa was achieved. Finally, samples were dried in an oven at 65°C for 48 h and weighed to determine dry mass and to calculate water released. Wood density ($\rho_{wood;}$ g cm^{-3}) was calculated as dry mass divided by fresh volume. Water released was plotted against Ψ_x and capacitance (C; kg m^{-3} MPa^{-1}) was determined by calculating the slope of the near linear portion in the initial part of the xylem water release curve. The range of the water potential in the initial part of the xylem water release curve was representative of the range of water potential that exhibited by the plants in the field.

Cuticular conductance

Three leaves were collected from each sample branch upon arrival to the laboratory. The cut end of the leaf was sealed with paraffin wax to limit the loss of water from the cut end so that water loss was limited to water lost through the stomata and the leaf cuticle. The samples were dried for a total of 4 h under outdoor ambient condition in the shade while measuring the mass of the leaf along with the humidity and temperature every 0.5 h. We assumed that the drying condition closed the stomata and thus resulted in water loss only through the cuticle. Cuticular conductance (g_{min}; mmol m^{-2} s^{-1}) was calculated by dividing the change in mass with the leaf area and the change in time for each interval. The value reported is the average of the g_{min} determined over the measurement interval.

Statistical analysis

Bivariate trait relationships were evaluated with Pearson product-moment correlation using the *Hmisc* package (Harrell Jr *et al.*, 2016) in *R* (R Core Team, 2016). The leverage potential of x-variable outliers was analyzed with the hat matrix procedure (Neter *et al.*, 1990). Phylogenetic independent contrasts (PICs) were calculated using the *ape* package (Paradis *et al.*, 2004) in *R*. The pruned tree was generated in phylocom (Webb & Donoghue, 2005) using the stored angiosperm tree (Zanne *et al.*, 2010). Principal components analysis (PCA) was done using the *prcomp* function in *R*, using the 10 traits measured in this study and 10 stem anatomical traits from the EcoFOG database (Fortunel *et al.*, 2014).

Results

The formation of vessel occlusions (*O* values) in this study ranged from no occurrence (-0.46 kg m^{-1} s^{-1} MPa^{-1} day^{-1}) to high expression (1.77 kg m^{-1} s^{-1} MPa^{-1} day^{-1}). Negative and near zero values of *O*, which indicate little to no formation of occlusions, were observed in *Bocoa prouacensis*, *Pradosia cochlearia, Jacaranda copaia, Symphonia globulifera, Eschweilera sagotiana, and Licania heteromorpha* listed in the order of increasing value. Other species produced occlusions which had a large impact on hydraulic conductivity, especially *Dicorynia guianensis* and *Lecythis persistens*.

Xylem hydraulic traits were highly variable among species. Capacitance (*C*) exhibited a 5.70-fold variation ranging from 83.40 kg m^{-3} MPa^{-1} in *L. heteromorpha* to 395 kg m^{-3} MPa^{-1} in *J. copaia*. Hydraulic transport efficiency ($K_{S\ max}$) exhibited a 9.48-fold variation among species, ranging from 0.71 kg m^{-1} s^{-1} MPa^{-1} in *L. heteromorpha* to 6.76 kg m^{-1} s^{-1} MPa^{-1} in *L. persistens*. Values for vulnerability segmentation (Ψ_D), which indicate the magnitude of change of leaf water potential per change in the stem water potential, ranged from -0.13 to 2.54. Two species, *Eperua falcata* and *J. copaia*, exhibited negative values indicating greatest drops in stem water potentials while maintaining stable leaf water potentials. Cavitation resistance (P_{50}) ranged between -1.05 MPa to -3.49 MPa where *E. falcata* exhibited the lowest xylem resistance and *B. prouacensis* exhibited the highest xylem resistance. Finally, cuticular conductance (g_{min}) exhibited a 6.81-fold variation among species, with *L. alba* exhibiting the highest g_{min} of 16.12 mmol m^{-2} s^{-1} and *E. sagotiana* exhibiting the lowest g_{min} with a water loss rate of 2.37 mmol m^{-2} s^{-1}.

Drought response traits were strongly correlated with one another when analyzed using either Pearson product-moment correlations or PIC, or both (Table 2.2). Among drought avoidance traits, *O* was positively correlated with *C* (r^2 = 0.59, *P* = 0.03; PIC r^2 = 0.99, *P* < 0.001; Table 2.2 and Fig. 2.1) suggesting that storage within the xylem may be related to the ability to form vessel occlusions and Ψ_D was negatively correlated with both *C* (PIC r^2 = -0.91, *P* < 0.001; Table 2.2) and *O* (PIC r^2 = -0.91, *P* < 0.001; Table 2.2), with species having greater leaf-stem water potential disequilibrium exhibiting greater xylem capacitance and high vessel occlusion formation rates. Drought avoidance traits were related to hydraulic transport: *O* was positively correlated with $K_{S\,max}$ (r^2 = 0.56, *P* = 0.04; PIC r^2 = 0.99, *P* < 0.001; Table 2.2 and Fig. 2.1), *C* was positively correlated with both $K_{S\,max}$ (r^2 = 0.64, *P* = 0.01; PIC r^2 = 0.99, *P* < 0.001; Table 2.2) and $K_{L\,max}$ (r^2 = 0.69, *P* = 0.007; Table 2.2), and Ψ_D was negatively related with both $K_{S\,max}$ (PIC r^2 = -0.88, *P* < 0.001; Table 2.2) and $K_{L\,max}$ (PIC r^2 = -0.61, *P* = 0.03; Table 2.2). Drought avoidance traits were also associated with hydraulic architecture traits: *O* was positively correlated with *LA:SA* (PIC r^2 = 0.90, *P* < 0.001; Table 2.2), *C* was positively correlated with *LA:SA* (PIC r^2 = 0.90, *P* < 0.001; Table 2.2), and Ψ_D was negatively related with *LA:SA* (PIC r^2 = -0.79, *P* = 0.001; Table 2.2).

Drought tolerance traits were correlated with one another for either Pearson product-moment correlations or PIC, or both (Table 2.2). Drought avoidance traits were correlated with drought tolerance: *C* was negatively correlated with ρ_{wood} (r^2 = - 0.79, *P* < 0.001; PIC r^2 = 0.99, *P* < 0.001; Table 2.2), P_e - P_{50} was negatively correlated with P_{50} (r^2 = - 0.73, *P* = 0.003; PIC r^2 = - 0.81, *P* < 0.001; Table 2.2), *O* was negatively

correlated with ρ_{wood} (PIC r^2 = - 0.88, $P < 0.001$; Table 2.2), and Ψ_D was positively correlated with g_{min} ($r^2 = 0.68$, $P = 0.008$; Table 2.2 and Fig. 2.2), P_{50} ($r^2 = 0.61$, $P =$ 0.02; Table 2.2 and Fig. 2.2), and ρ_{wood} (PIC $r^2 = 0.91$, $P < 0.001$; Table 2.2). There were negative correlations between drought tolerance with both architecture and transport traits: ρ_{wood} with *LA:SA* (PIC r^2 = -0.87, $P < 0.001$; Table 2.2), $K_{L\,max}$ (r^2 = -0.84, $P <$ 0.001; PIC r^2 = -0.58, $P = 0.04$; Table 2.2), and $K_{S\,max}$ (PIC r^2 = -0.97, $P < 0.001$; Table 2.2). In addition to the relationship of transport with drought avoidance and drought resistance, $K_{S\,max}$ was positively correlated with both $K_{L\,max}$ ($r^2 = 0.65$, $P = 0.01$; Table 2.2) and *LA:SA* (PIC $r^2 = 0.91$, $P < 0.001$; Table 2.2).

A principle components analyses showed the relationships between these many traits. The first PCA axis accounted for 34.2% of the variance and was largely associated with xylem storage (Fig. 2.3). The highest absolute eigenvector scores for the negative range of the first PCA axis were parenchyma fraction and lumen fraction whereas wood specific gravity and vessel grouping index loaded on the positive range of the first PCA axis. The second PCA axis accounted for 22.2% of the variance and was largely associated with xylem hydraulic transport (Fig. 2.3). The highest absolute eigenvector scores for the negative range of the second PCA axis were vessel fraction and vessel density whereas stem vessel size to number ratio and mean vessel area loaded on the positive range of the second PCA axis.

Discussion

The formation of vessel occlusions within the xylem appears to be associated with the ability of plants to avoid drought. This is linked to the role of occlusions in increased transport resistance in the terminal branches as dehydration progressed for some species (Fig. 2.1 and 2.6). The increased resistance was due to irreversible declines in transport that resulted in increased segmentation of the plant and this was evident in increased water potential gradients.

Our results are consistent with other studies that have examined vessel occlusion formation. For instance, similar to our study, another study found that flushing stems after the onset of gels did not restore the maximum hydraulic conductivity and that the amount of occlusions within large branches increased over the course of multi-day dehydration (Jacobsen & Pratt, 2012). Our study also found evidence that links vessel occlusion formation to the parenchyma fractions and lumen fraction of the xylem (Figure 2.3). Previous studies have linked vessel occlusions to anatomical structures such as the parenchyma fraction and lumen size (De Micco *et al.*, 2016) and many studies have examined the link between hydraulic function and vessel occlusion formation in the context of pathogens; however, there have been very few studies that have directly tested the relationship between vessel occlusion formation and hydraulic functioning in the context of drought traits in tropical forests. A possible explanation could be due to the underrepresentation of hydraulic studies from tropical biomes, which accounted for less than a third of global data (Choat *et al.*, 2012). Vessel occlusion formations are more likely expressed in tropical trees because of the high frequency of axial xylem

parenchyma relative to temperate trees (Morris *et al.*, 2015). The importance of anatomical contribution, or absence, to hydraulic function is key to understand adjustments in hydraulic transport along the soil-plant-atmosphere-continuum. For example, transgenic poplars with low lignin content have been shown to have reduced water transport due to vessel occlusion (Kitin *et al.*, 2010) hinting at an alternative way to increase transport resistance other than narrow xylem vessels. Linking vessel occlusion to drought strategies could help explain why plants with highly vulnerable xylem can persist despite a drying environment.

An alternative explanation for the selection for vessel occlusion formation in some species may be as a defense response. On the one hand, selection for high wood density has been suggested for tropical species as a defense mechanism against wood pathogens (Auspurger & Kelly, 1984). In the other hand, species with low wood density as a consequence of the evolution of efficient hydraulic transport may have developed the ability to form occlusion as an alternative defensive pathway (Bonsen & Kučera, 1990). For species that form vessel occlusions that are simultaneously vulnerable to hydraulic transport failure, formation of occlusions may be a necessary means of blocking embolised vessels from becoming pathways of pathogen entry into plants that are already weakened by hydraulic failure. The contrasting impacts of a hydraulic axis of variation and a defense axis of variation are beyond the scope of this study, and thus require further investigation.

The formation of vessel occlusions is linked to the pit pore sizes in the membrane that divides vessels from adjoining contact cells, which are specialized ray parenchyma

cells that connect with adjacent vessel elements by half-bordered pit pairs (Braun, 1967). Tyloses fill a vessel through outgrowths of contact cells that push through the pits (Zimmermann, 1979) and tyloses generally develop in vessel-ray parenchyma pit pairs that have an aperture greater than 10 μm (Bonsen & Kučera, 1990). Furthermore, tyloses can lignify and contain secondary metabolite deposits (Chattaway, 1949). Both of the terms gums and gels (as well as some additional terms) have been used to indicate types of occlusions that contain polysaccharides and pectin (De Micco *et al.*, 2016), however the term gel was proposed for use in pectin occlusions secreted from parenchyma cells into vessels (Rioux 1998). Gels fill a vessel through secretion through the pits from contact cells which generally develop in vessel-ray parenchyma pit aperture less than 10 μm (Bonsen & Kučera, 1990). It is currently accepted that occlusion formation is often preceded by embolism formation, thus many biotic and abiotic factors that affect embolism formation may indirectly affect of occlusion formation(De Micco *et al.*, 2016).

In the context of this study, it is most likely that occlusions formed as a result of dehydration and not from wounding or pathogen because the subsamples were collected about 1 m distal from the cut end and well away from where the wound response would likely be active. It is possible that pathogens could have impacted dehydrated braches, but since all branches were treated the same, this would not account for the differences in occlusion formation between species. Unfortunately we cannot discern whether reductions in hydraulic conductivity were to specific types of occlusions, because we did not conduct microscopic analysis of our specimens.

Our data indicate that the rate of occlusion formation was positively correlated to capacitance which buffers diurnal changes in water potential and also positively correlated with $K_{S\ max}$ where higher rates of transport coincided with high rates of occlusion formation. The reduction conductivity in relation to vessel occlusion was consistent with other studies (Salleo and Lo Gullo, 1989, Sano and Fukazawa 1991, Jacobsen and Pratt 2012). A strong coordination among drought avoidance traits was observed where vessel occlusion formation was positively correlated with capacitance (Fig. 2.2, Table 2.2) and both traits traded-off with Ψ_D, with higher values indicating greater levels of water potential disequilibrium between leaf and stem. The correlations among these traits indicate a strong ability to maximize hydraulic resources for leaf gas exchange (Santiago *et al.*, 2004a) while also having an adjustment mechanism to prevent run-away cavitation. Capacitance is the first of the adjustments to occur and has been linked to buffering the effects of variable demand by transpiration on gas exchange (Meinzer *et al.*, 2003, 2009; Gleason *et al.*, 2014), where the source of the released water is due to the effect of cavitation induction in water filled vessels (Tyree & Zimmermann, 2002; Hölttä *et al.*, 2009). Hydraulic segmentation in the form of vessel occlusion is the next to occur, either due to ethylene production as the drought progresses (Sun *et al.*, 2007) or after cavitation (Jacobsen & Pratt, 2012). Finally, when transpiration resources are low a strong disequilibrium between the leaf and stem water potential are created that later result in drought deciduousness (Santiago *et al.*, 2016; Wolfe *et al.*, 2016). Wolfe *et al.* (2016) pointed out that leaf shedding is not universally effective in preventing further desiccation in plants, thus there is a strong potential for the hydraulic segmentation

capacity of vessel occlusion to further limit transpiration. This remains to be further tested.

There is evidence to support the trade-off between drought avoidance traits and drought tolerance traits (Fig. 2.2, Table 2.2). Furthermore, drought avoidance traits were correlated with high transport rates and greater LA:SA (Fig. 2.1, Table 2.2). This result reflects what has been found in the safety-efficiency trade-off (Maherali *et al.*, 2004; Gleason *et al.*, 2015). However our finding highlights the mechanisms that promote changes in hydraulic resistance as water potential declines. Adjustment in hydraulic resistance and the formation of occlusions may safeguard cavitated vessels from nucleating additional cavitation events either through capacitance of water stored in xylem vessels or through changing locations of air-water menisci.

The orthogonal axes that appear in the PCA capture the trade-off between drought avoidance and drought tolerance and also the trade-off between few wide diameter vessels and many packed small diameter vessels (Fig. 2.3). The loading of *C* with $K_{S\,max}$ is consistent with other published work where *C* was able to influence water transport (Goldstein *et al.*, 1998; Meinzer *et al.*, 2003, 2008). Furthermore, the strong loading of *C* with lumen fraction and parenchyma fraction is consistent with the cavitation release of water from the vessel lumen and extraxylary components of water transport (Zimmermann, 1983; Holbrook, 1995; Nolf *et al.*, 2015). It is not surprising to see *O* loading with *C* and $K_{S\,max}$ given that it directly influences both traits (Fig. 2.1); however it is interesting to note that *O* loaded with both lumen fraction and parenchyma fraction because both anatomical traits are directly involved in the development of vessel

occlusion in the xylem vessels (De Micco *et al.*, 2016). Perhaps the loading of *O* is related to the relationship between transport and storage in xylem function (Pratt & Jacobsen, 2016). The loading of P_{50} with wood specific gravity (WSG) was consistent with what have been found in other studies where fibers are strong determinant of WSG (Fortunel *et al.*, 2014) and also influence cavitation resistance (Jacobsen *et al.*, 2005). The g_{min} and the vulnerability segmentation trait Ψ_D are leaf related traits involved in water management and these traits loaded strongly with fiber fraction. Perhaps the greater proportion of fiber fraction enables fewer investments to prevent leakiness in leaves. In a study on vulnerability segmentation, Wolfe *et al.* (2016) pointed out that drought deciduousness alone does not prevent further loss of water for some species, therefore fiber fractions may interact with this and this idea deserves further consideration. The loading of LA:SA with vessel size to number ratio and mean vessel area is also consistent with supply-demand of water in leaves where greater leaf area require greater hydraulic demand. Overall, the loading of the hydraulic traits with anatomy traits links function with structure and highlights the need to further investigate certain traits.

The increase in observed plant mortality across the globe (Allen *et al.*, 2010; Anderegg *et al.*, 2015) calls for the need to investigate interacting hydraulic physiological mechanisms that promote plant survival during drought. Our study suggests that plants utilize coordinated drought response traits to cope with water deficit. The coordination of drought avoidance traits may be a mechanism to explain the global finding that many plants operate close to their hydraulic limits (Choat *et al.*, 2012), as it offers an alternative view of a more resilient hydraulic pipeline. Our results suggest that hydraulic

segmentation, vulnerability segmentation, and capacitance are coordinated and allow maximization of water transport and adjustments during water deficit. Furthermore, our findings implicate the living xylem fractions in modulating transport, expanding our notion of passive transport of water through the conductive path.

References

Allen CD, Macalady AK, Chenchouni H, Bachelet D, McDowell NG, Vennetier M, Kitzberger T, Rigling A, Breshears DD, Hogg EH (Ted), *et al.* 2010. A global overview of drought and heat-induced tree mortality reveals emerging climate change risks for forests. *Forest Ecology and Management* **259**: 660–684.

Anderegg WRL, Hicke JA, Fisher RA, Allen CD, Aukema J, Bentz B, Hood S, Lichstein JW, Macalady AK, McDowell N, *et al.* 2015. Tree mortality from drought, insects, and their interactions in a changing climate. *New Phytologist*.

Auspurger CK, Kelly CK. **1984**. Pathogen mortality of tropical seedlings: experimental studies of the effects of dispersal distance, seedling density, and light conditions. *Oecologia* **61**: 211-217.

Bartlett MK, Zhang Y, Kreidler N, Sun S, Ardy R, Cao K, Sack L. **2014**. Global analysis of plasticity in turgor loss point, a key drought tolerance trait. *Ecology Letters* **17**: 1580–1590.

Bonsen KJM, Kučera LJ. **1990**. Vessel occlusions in plants: morphological, functional and evolutionary aspects. *Iawa Bulletin n. s.* **11**: 393–399.

Borchert R, Pockman WT. **2005**. Water storage capacitance and xylem tension in isolated branches of temperate and tropical trees. *Tree physiology* **25**: 457–66.

Braun HJ. **1967**. Development and structure of wood rays in view of contact-isolation-differentiation to hydrostem. *Holzforschung* **21**: 33-37.

Chattaway MM. **1949**. The development of tyloses and secretion of gum in heartwood formation. *Australian Journal of Sicentific Research, Series B, Biological Sciences* **2**: 227–249.

Chaves MM, Maroco JP, Pereira JS. **2003**. Understanding plant responses to drought — from genes to the whole plant. *Functional Plant Biology*: 239–264.

Choat B, Jansen S, Brodribb TJ, Cochard H, Delzon S, Bhaskar R, Bucci SJ, Feild TS, Gleason SM, Hacke UG, *et al.* 2012. Global convergence in the vulnerability of forests to drought. *Nature* **491**: 752–5.

Choat B, Pittermann J. **2009**. New insights into bordered pit structure and cavitation resistance in angiosperms and conifers. *New phytologist* **182**: 557–560.

De Micco V, Balzano A, Wheeler EA, Baas P. **2016**. A review of structure, function and occurrence of vessel occlusion. *IAWA Journal* **37**: 186-205.

Dixon H, Joly J. **1895**. On the ascent of sap. *Philosophical Transactions of the Royal Society of London* **186**: 563–576.

Fortunel C, Ruelle J, Beauchêne J, Fine PVA, Baraloto C. **2014**. Wood specific gravity and anatomy of branches and roots in 113 Amazonian rainforest tree species across environmental gradients. *New Phytologist* **202**: 79–94.

Gleason SM, Blackman CJ, Cook AM, Laws CA, Westoby M. **2014**. Whole-plant capacitance, embolism resistance and slow transpiration rates all contribute to longer desiccation times in woody angiosperms from arid and wet habitats. *Tree physiology* **34**: 275–84.

Gleason SM, Westoby M, Jansen S, Choat B, Hacke UG, Pratt RB, Bhaskar R, Brodribb TJ, Bucci SJ, Cao K, *et al.* 2015. Weak tradeoff between xylem safety and xylem-specific hydraulic efficiency across the world s woody plant species. *New Phytologist* **209**: 123–136.

Goldstein G, Andrade JL, Meinzer FC, Holbrook NM, Cavelier J, Jackson P. **1998**. Stem water storage and diurnal patterns of water use in tropical forest canopy trees. *Plant, Cell and Environment* **21**: 397–406.

Guehl J-M, Bonal D, Ferhi A, Barigah TS, Farquhar G, Granier a BT-E and M of a NR. **2004**. *Ecology and Management of a Neotropical Rainforest*. Elsevier.

De Guzman ME, Santiago LS, Schnitzer S, Álvarez-Cansino L. **2016**. Trade-offs between water transport capacity and drought resistance in neotropical canopy liana and tree species. *Tree Physiology*.

Hacke UG, Stiller V, Sperry JS, Pittermann J, McCulloh K a. **2001**. Cavitation fatigue. Embolism and refilling cycles can weaken the cavitation resistance of xylem. *Plant physiology* **125**: 779–86.

Hao GY, Hoffmann WA, Scholz FG, Bucci SJ, Meinzer FC, Franco AC, Cao KF, Goldstein G. **2008**. Stem and leaf hydraulics of congeneric tree species from adjacent tropical savanna and forest ecosystems. *Oecologia* **155**: 405–415.

Harrell Jr FE, Dupont C, Al. E. **2016**. Hmisc: Harrell Miscellaneous.

Holbrook N. **1995**. Stem water storage. In: Gartner B, ed. Plant Stems: Physiology and Functional Morphology. San Diego: Academic Press, 151–174.

Hölttä T, Cochard H, Nikinmaa E, Mencuccini M. **2009**. Capacitive effect of cavitation in xylem conduits: results from a dynamic model. *Plant, cell & environment*

32: 10–21.

Jacobsen AL, Ewers FW, Pratt RB. **2005**. Do xylem fibers affect vessel cavitation resistance? *Plant Physiology* **139**: 546–556.
Jacobsen AL, Pratt RB. **2012**. No evidence for an open vessel effect in centrifuge-based vulnerability curves of a long-vesselled liana (Vitis vinifera). *The New phytologist* **194**: 982–90.

Kitin P, Voelker SL, Meinzer FC, Beeckman H, Strauss SH, Lachenbruch B. **2010**. Tyloses and phenolic deposits in xylem vessels impede water transport in low-lignin transgenic poplars: a study by cryo-fluorescence microscopy. *Plant physiology* **154**: 887–98.

Klein G. **1923**. Zur Aetiologie der Thyllen. **15**: 418–439.

Lens F, Sperry JS, Christman MA, Choat B, Rabaey D, Jansen S. **2011**. Testing hypotheses that link wood anatomy to cavitation resistance and hydraulic conductivity in the genus Acer. *New Phytologist* **190**: 709–723.

Levitt JBT-R of plants to environmental stresses. **1972**. *Responses of plants to environmental stresses*. New York, San Francisco, London: Academic Press.

Maherali H, Pockman WT, Jackson RB. **2004**. Adaptive variation in the vulnerability of woody plants to xylem cavitation. *Ecology* **85**: 2184–2199.

Maréchaux I, Bartlett MK, Sack L, Baraloto C, Engel J, Joetzjer E, Chave J. **2015**. Drought tolerance as predicted by leaf water potential at turgor loss point varies strongly across species within an Amazonian forest. *Functional Ecology* **29**: 1268-1277.

McCulloh KA, Johnson DM, Meinzer FC, Woodruff DR. **2014**. The dynamic pipeline: hydraulic capacitance and xylem hydraulic safety in four tall conifer species. *Plant, Cell and Environment* **37**: 1171–83.

Meinzer FC, James SA, Goldstein G, Woodruff D. **2003**. Whole-tree water transport scales with sapwood capacitance in tropical forest canopy trees. *Plant, Cell and Environment* **26**: 1147–1155.

Meinzer FC, Johnson DM, Lachenbruch B, McCulloh KA, Woodruff DR. **2009**. Xylem hydraulic safety margins in woody plants: Coordination of stomatal control of xylem tension with hydraulic capacitance. *Functional Ecology* **23**: 922–930.

Meinzer FC, Woodruff DR, Domec J-C, Goldstein G, Campanello PI, Gatti MG, Villalobos-Vega R. **2008**. Coordination of leaf and stem water transport properties in tropical forest trees. *Oecologia* **156**: 31–41.

Morris H, Plavcova L, Cvecko P, Fichtler E, Gillingham MAF, Martinez-Cabrera HI, McGlinn DJ, Wheeler E, Zheng J, Zieminska K, *et al.* 2015. A global analysis of parenchyma tissue fractions in secondary xylem of seed plants. *New Phytologist*: 1553–1565.

Naidoo S, Zboňák A, Ahmed F. **2006**. The effect of moisture availability on wood density and vessel characteristics of Eucalyptus grandis in the warm temperate region of South Africa. In: Kurjatko S,, In: Kúdela J,, In: Lagana R, eds. Proceedings of the 5th International Symposium on Wood Structure and Properties. Zvolen, Slovakia: Arbora Publishers, 117–122.

Neter J, Wasserman W, Kunter M. **1990**. *Applied linear statistical models*. Irwin, Boston.

Nolf M, Creek D, Duursma R, Holtum J, Mayr S, Choat B. **2015**. Stem and leaf hydraulic properties are finely coordinated in three tropical rain forest tree species. *Plant, Cell and Environment* **38**: 2652–2661.

Oliva Carrasco L, Bucci SJ, Di Francescantonio D, Lezcano OA, Campanello PI, Scholz FG, Rodriguez S, Madanes N, Cristiano PM, Hao G-Y, *et al.* 2014. Water storage dynamics in the main stem of subtropical tree species differing in wood density, growth rate and life history traits. *Tree Physiology*: 354–365.

Paradis E, Claude J, Strimmer K. **2004**. APE: analyses of phylogenetics and evolution in R language. *Bioinformatics* **20**: 289–290.

Phillips N, Oren R, Zimmermann R, Wright SJ. **1999**. Temporal patterns of water flux in trees and lianas in a Panamanian moist forest. *Trees* **14**: 116.

Pivovaroff AL, Sack L, Santiago LS. **2014**. Coordination of stem and leaf hydraulic conductance in southern California shrubs: a test of the hydraulic segmentation hypothesis. *New Phytologist* **203**: 842–50.

Pratt RB, Jacobsen AL. **2016**. Conflicting demands on angiosperm xylem: tradeoffs among storage, transport, and biomechanics. *Plant, Cell and Environment*.

Pratt RB, Jacobsen AL, Ewers FW, Davis SD. **2007**. Relationships among xylem transport, biomechanics and storage in stems and roots of nine Rhamnaceae species of the California chaparral. *New Phytologist* **174**: 787–98.

R Core Team. **2016**. R: A language and environment for statistical computing.

Richards AE, Wright IJ, Lenz TI, Zanne AE. **2014**. Sapwood capacitance is greater in

evergreen sclerophyll species growing in high compared to low-rainfall environments (M Tjoelker, Ed.). *Functional Ecology* **28**: 734–744.

Rickard JE, Marriott J. **1979**. Occlusions in Cassava Xylem Vessels Associated with Vascular Discoloration. *Annals of botany*: 523–526.

Rioux D, Nicole M, Simard M, Ouellette GB. **1998**. Immunocytochemical evidence that secretion of pectin occurs during gel (gum) and tylosis formation in trees. *Phytopathol* **6**: 494-505.

Salleo S, Lo Gullo MA. **1989**. Xylem cavitation in nodes and internodes of *Vitis vinifera* L. plant subjected to water stress. Limits of restoration of water conduction in cavitated xylem conduits. In: Kreeb KH, Richter H, Hinckley TM (eds.), Structural and Functional Responses to Environmental Stress: 32-42. SPB Academic Publishing.

Sano Y, Fukazawa K. **1991**. Structural differences of tyloses in *Fraxinus mandshurica* var. *japonica* and *Kalopanax pictus*. *IAWA* **12**: 241-9.

Santiago LS, Bonal D, De Guzman ME, Ávila-Lovera E. **2016**. Drought survival strategies of tropical trees. In: Goldstein G, Santiago LS, eds. Tropical Tree Physiology. Switzerland: Springer, 243–258.

Santiago LS, Goldstein G, Meinzer FC, Fisher JB, Machado K, Woodruff D, Jones T. **2004**. Leaf photosynthetic traits scale with hydraulic conductivity and wood density in Panamanian forest canopy trees. *Oecologia* **140**: 543–550.

Scholz FG, Bucci SJ, Goldstein G, Meinzer FC, Franco AC, Miralles-Wilhelm F. **2007**. Biophysical properties and functional significance of stem water storage tissues in Neotropical savanna trees. *Plant, Cell and Environment* **30**: 236–48.

Skelton RP, West AG, Dawson TE. **2015**. Predicting plant vulnerability to drought in biodiverse regions using functional traits. *Proceedings of the National Academy of Sciences* **112**: 5744-5749.

Sperry JS. **1986**. Relationship of Xylem Embolism to Xylem Pressure Potential, Stomatal Closure, and Shoot Morphology in the Palm Rhapis excelsa. *Plant physiology* **80**: 110–116.

Sperry JS, Donnelly JR, Tyree MT. **1988**. A method for measuring hydraulic conductivity and embolism in xylem. *Plant, Cell and Environment* **11**: 35–40.

Stahl C, Hérault B, Rossi V, Burban B, Bréchet C, Bonal D. **2013**. Depth of soil water uptake by tropical rainforest trees during dry periods: Does tree dimension matter? *Oecologia* **173**: 1191–1201.

Sun Q, Rost TL, Reid MS, Matthews MA. 2007. Ethylene and not embolism is required for wound-induced tylose development in stems of grapevines. *Plant Physiology* **145**: 1629-36.
Sun Q, Rost TL, Matthews MA. **2008**. Wound-induced vascular occlusions in *Vitis vinifera* (Vitaceae): tyloses in summer and gels in winter. *American Journal of Botany* **95**: 1498–505.

Tyree M, Cochard H, Cruiziat P, Sinclair B, Ameglio T. **1993**. Drought-induced leaf shedding in walnut: evidence for vulnerability segmentation. *Plant, Cell and Environment* **16**: 879–882.

Tyree M, Ewers F. **1991**. The hydraulic architecture of trees and other woody plants. *New Phytologist* **119**: 345–360.

Tyree M, Zimmermann M. **2002**. *Xylem structure and the ascent of sap*. Berlin, Heidelberg, Germany, New York, NY, USA: Springer.

Vergeynst LL, Dierick M, Bogaerts JAN, Cnudde V, Steppe K. **2014**. Cavitation: a blessing in disguise? New method to establish vulnerability curves and assess hydraulic capacitance of woody tissues. *Tree Physiology*: 1–10.

Wagner F, Hérault B, Stahl C, Bonal D, Rossi V. **2011**. Modeling water availability for trees in tropical forests. *Agricultural and Forest Meteorology* **151**: 1202–1213.

Webb CO, Donoghue M. **2005**. Phylomatic: tree assembly for applied phylogenetics. *Molecular Ecology Notes* **5**: 181–183.

Westoby M, Wright IJ. **2006**. Land-plant ecology on the basis of functional traits. *Trends in Ecology and Evolution* **21**: 261–8.

Wheeler JK, Sperry JS, Hacke UG, Hoang N. **2005**. Inter-vessel pitting and cavitation in woody Rosaceae and other vesselled plants: A basis for a safety versus efficiency trade-off in xylem transport. *Plant, Cell and Environment* **28**: 800–812.

Whitehead D, Edwards WRN, Jarvis PG. **1984**. Conducting sapwood area, foliage area and permeability in mature trees of *Picea sitchensis* and *Pinus contorta*. *Canadian Journal of Forest Research* **14**: 940-947.

Wolfe BT, Kursar TA. **2015**. Diverse patterns of stored water use among saplings in seasonally dry tropical forests. *Oecologia* **179**: 925–936.

Wolfe BT, Sperry JS, Kursar TA. **2016**. Does leaf shedding protect stems from cavitation during seasonal droughts? A test of the hydraulic fuse hypothesis. *New*

Phytologist **212**: 1007-1018

Zanne AE, Westoby M, Falster DS, Ackerly DD, Loarie SR, Arnold SEJ, Coomes D a. **2010**. Angiosperm wood structure: Global patterns in vessel anatomy and their relation to wood density and potential conductivity. *American journal of botany* **97**: 207–215.

Zhao XH, Liu LY, Nan LJ, Wang H, Li H. **2014**. Development of tyloses in the xylem vessels of Meili grapevine and their effect on water transportation. *Russian Journal of Plant Physiology* **61**: 194–203.

Zimmermann MH. **1979**. Discovery of Tylose Formation By a Viennese Lady in 1845. *Iawa Bulletin*: 51.

Zimmermann M. **1983**. *Xylem structure and the ascent of sap*. New York: Springer-Verlag.

Tables and Figures

Table 2.1. Plant species, family, and symbol

Species	Family	Symbol
Bocoa prouacensis	Fabaceae	
Dicorynia guianensis	Fabaceae	
Eperua falcata	Fabaceae	
Eperua grandiflora	Fabaceae	
Eschweilera sagotiana	Lecythidaceae	
Jacaranda copaia	Bignoniaceae	
Lecythis persistens	Lecythidaceae	
Licania alba	Chrysobalanaceae	
Licania heteromorpha	Chrysobalanaceae	
Pradosia cochlearia	Sapotaceae	
Sextonia rubra	Lauraceae	
Symphonia globulifera	Clusiaceae	
Tachigali melinonii	Fabaceae	
Vouacapoua americana	Fabaceae	

Table 2.2. Pearson product-moment correlation coefficients (r) for species traits are listed in the upper right half of the matrix (n = 14). Correlation coefficients for phylogenetically independent contrasts are listed in the lower left half of the matrix (n = 14). Bold type indicates significant correlations ($P \leq 0.05$).

	Ψ_D	g_{min}	C	ρ_{wood}	P_{50}	P_e	$P_e - P_{50}$	$K_{S\,max}$	$K_{L\,max}$	$LA:SA$	O
Ψ_D		**0.679**	-0.424	0.439	**0.605**	0.413	-0.330	-0.342	-0.350	-0.153	-0.127
g_{min}	0.485		-0.408	0.369	0.512	0.421	-0.225	-0.491	-0.443	-0.122	-0.019
C	**-0.907**	-0.285		**-0.793**	-0.090	-0.089	0.029	**0.644**	**0.687**	0.105	**0.587**
ρ_{wood}	**0.908**	0.278	**-0.992**		0.089	0.105	-0.015	-0.454	**-0.840**	0.166	-0.149
P_{50}	-0.203	0.262	0.496	-0.508		0.447	**-0.728**	-0.035	0.053	-0.215	0.043
P_e	-0.061	0.198	0.160	-0.156	0.473		0.288	-0.418	-0.154	-0.514	0.125
$P_e - P_{50}$	0.220	-0.097	-0.477	0.487	**-0.814**	0.114		-0.283	-0.175	-0.164	0.050
$K_{S\,max}$	**-0.881**	-0.296	**0.987**	**-0.972**	0.500	0.072	-0.544		**0.651**	0.142	**0.561**
$K_{L\,max}$	**-0.606**	-0.454	0.511	**-0.577**	0.281	0.217	-0.188	0.421		-0.388	0.131
$LA:SA$	**-0.786**	-0.276	**0.896**	**-0.865**	0.407	-0.015	-0.491	**0.905**	0.323		0.141
O	**-0.877**	-0.216	**0.990**	**-0.972**	0.520	0.155	-0.506	**0.991**	0.398	**0.903**	

Symbol legend: $\Psi_{leaf} - \Psi_{stem}$ disequilibrium (Ψ_D; MPa MPa^{-1}), leaf cuticular conductance(g_{min}; mmol m^{-2} s^{-1}), capacitance (C; kg m^{-3} MPa^{-1}), wood density (ρ_{wood}; g cm^{-3}), 50 percent loss in conductivity (P_{50}; MPa), air entry threshold (P_e; MPa), steepness of vulnerability curve ($P_e - P_{50}$; MPa), stem-specific maximum hydraulic conductivity ($K_{S\,max}$; kg m^{-1} s^{-1} MPa^{-1}), leaf-specific maximum hydraulic conductivity ($K_{L\,max}$; kg m^{-1} s^{-1} MPa^{-1}), leaf area to sapwood area ratio ($LA:SA$; m^2 m^{-2}), and vessel occlusion (O; kg m^{-1} s^{-1} MPa^{-1} day^{-1}).

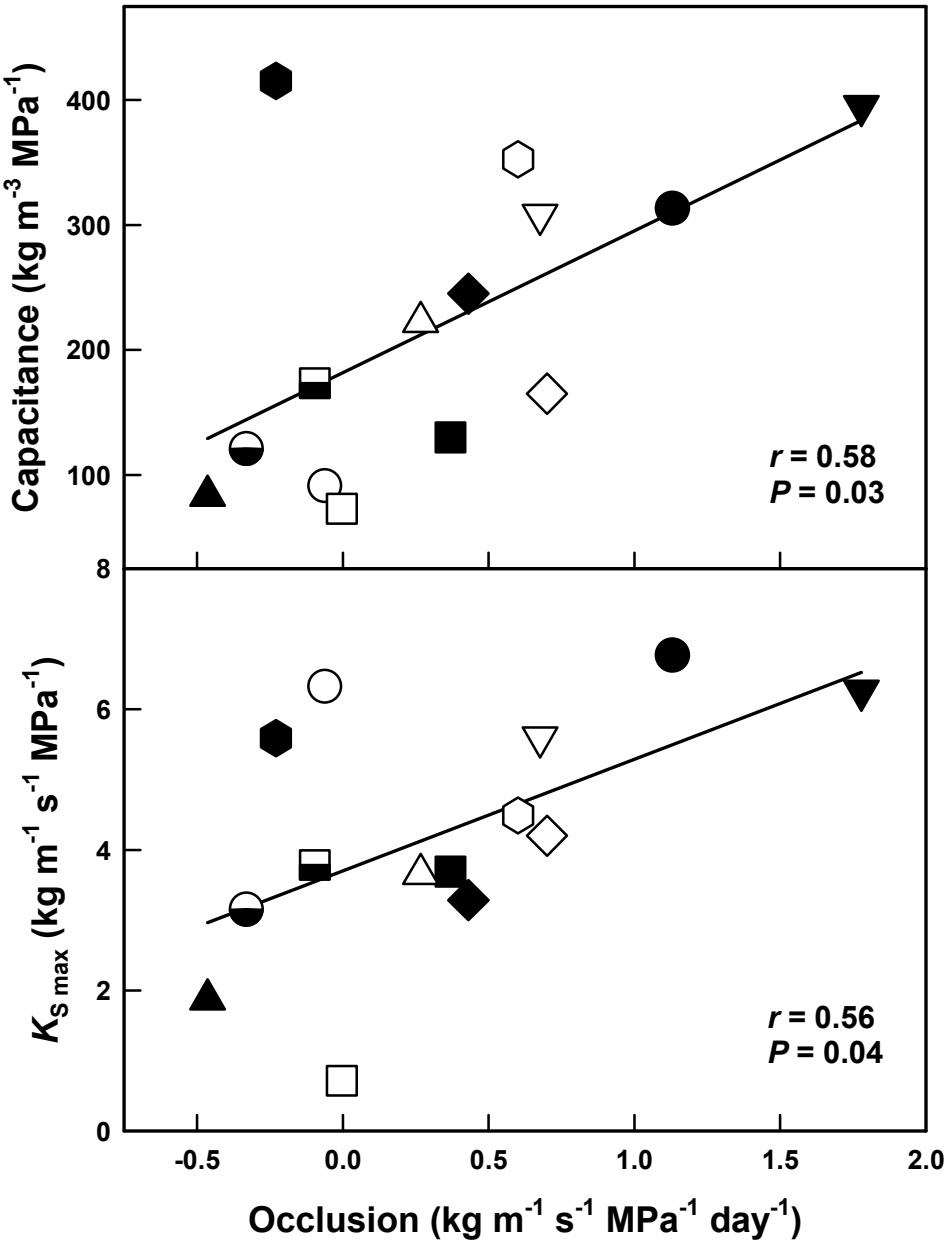

Figure 2.1. The relationship of occlusion with capacitance (*top*) and $K_{S\,max}$ (*bottom*) for 14 Amazonian canopy rainforest tree species sampled from the research plots in Paracou, French Guiana. Best fit line from Pearson correlations are drawn in solid line. The symbols corresponds to the study species as indicated in Table 1.

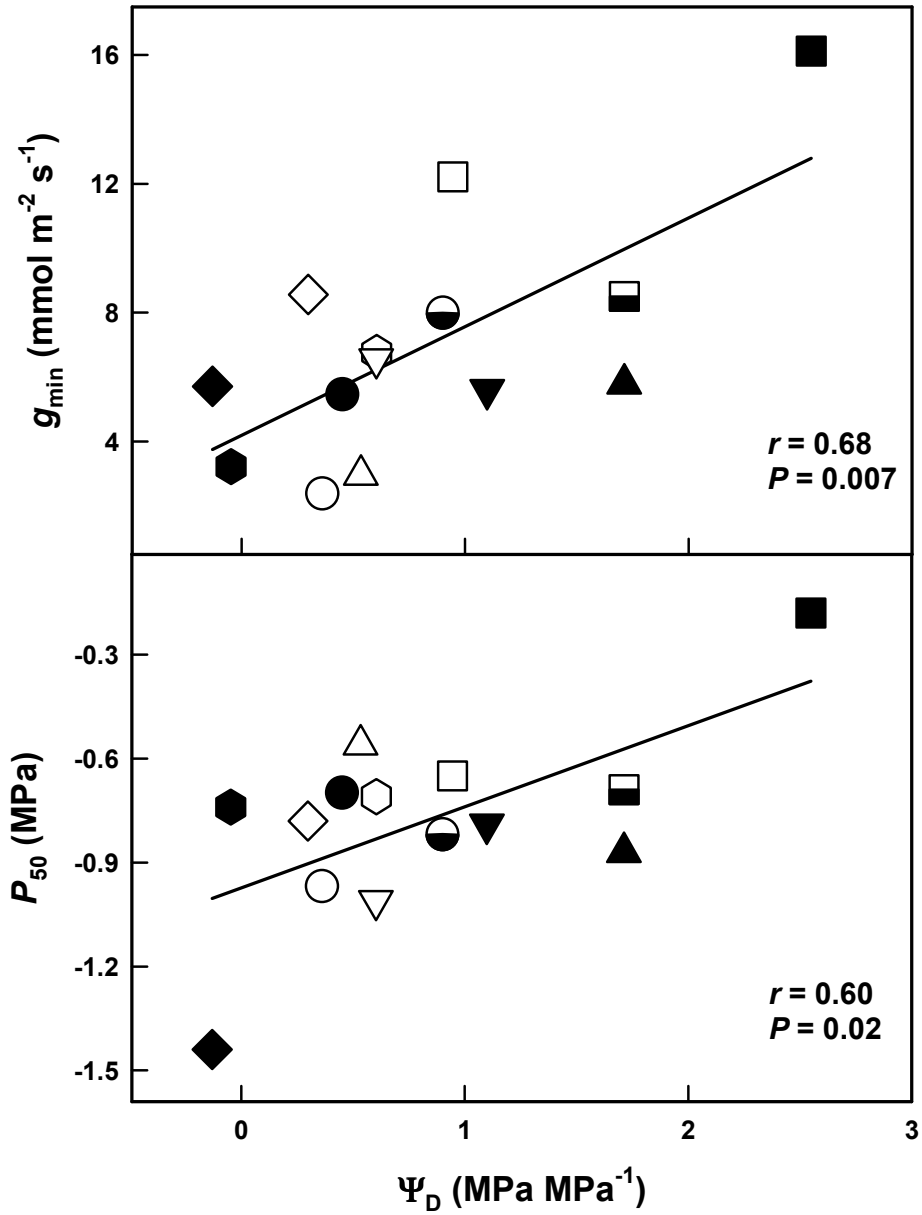

Figure 2.2. The relationship of $\Psi_{leaf} - \Psi_{stem}$ disequilibrium (Ψ_D) with cuticular conductance (g_{min}; *top*) and resistance to cavitation (P_{50} ;*bottom*) for 14 Amazonian canopy rainforest tree species sampled from the research plots in Paracou, French Guiana. Best fit line from Pearson correlations are drawn in solid line. The symbols corresponds to the study species as indicated in Table 1.

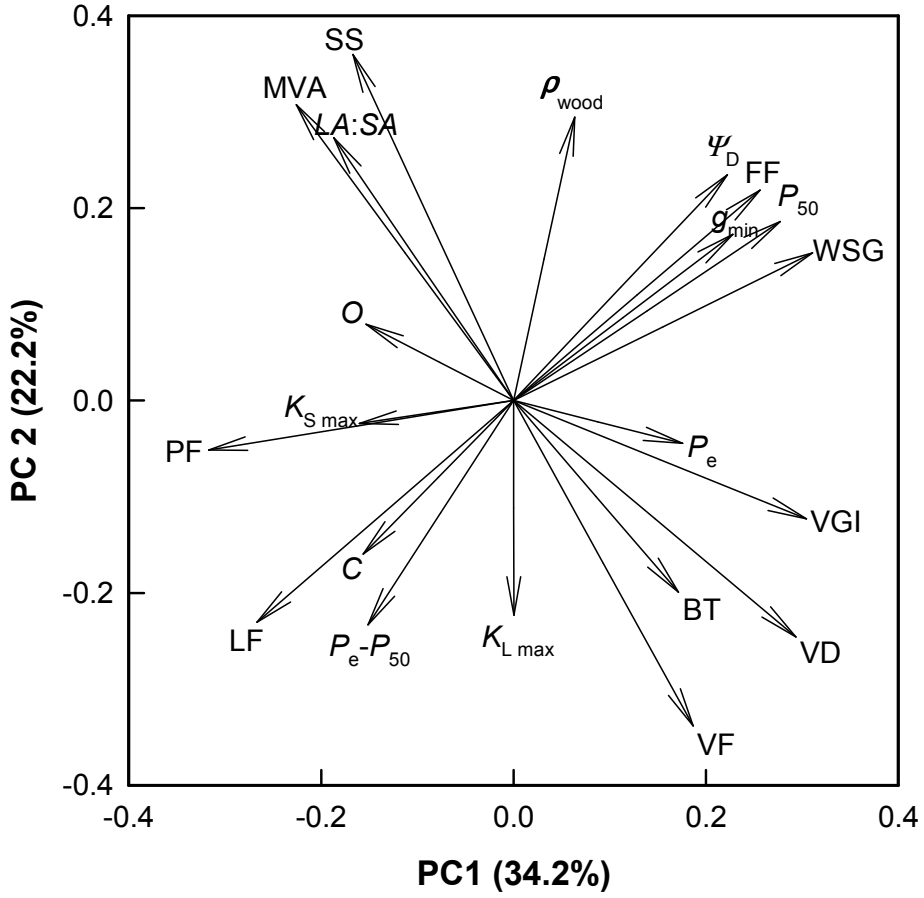

Figure 2.3. Principal component analysis ordination for 11 hydraulic traits measured during this study and 10 anatomical traits extracted from EcoFOG database. *Hydraulic traits legend*: $\Psi_{leaf} - \Psi_{stem}$ disequilibrium (Ψ_D; MPa MPa^{-1}), leaf cuticular conductance(g_{min}; mmol m^{-2} s^{-1}), capacitance (C; kg m^{-3} MPa^{-1}), wood density (ρ_{wood}; g cm^{-3}), 50 percent loss in conductivity (P_{50}; MPa), air entry threshold (P_e; MPa), steepness of vulnerability curve (P_e - P_{50}; MPa), stem-specific maximum hydraulic conductivity ($K_{S\ max}$; kg m^{-1} s^{-1} MPa^{-1}), leaf-specific maximum hydraulic conductivity ($K_{L\ max}$; kg m^{-1} s^{-1} MPa^{-1}), leaf area to sapwood area ratio (*LA:SA*; m^2 m^{-2}), and vessel occlusion (O; kg m^{-1} s^{-1} MPa^{-1} day^{-1}). *Anatomical traits legend*: bark thickness (BT; cm), fiber fraction (FF, no unit), lumen fraction (LF; no unit), mean vessel area (MVA; μm^2), parenchyma fraction (PF; no unit), vessel size to number ratio (SS; μm^4), vessel density (VD; μm^{-2}), vessel fraction (VF; no unit), vessel group index (VGI; no unit), and wood specific gravity (WSG; no unit).

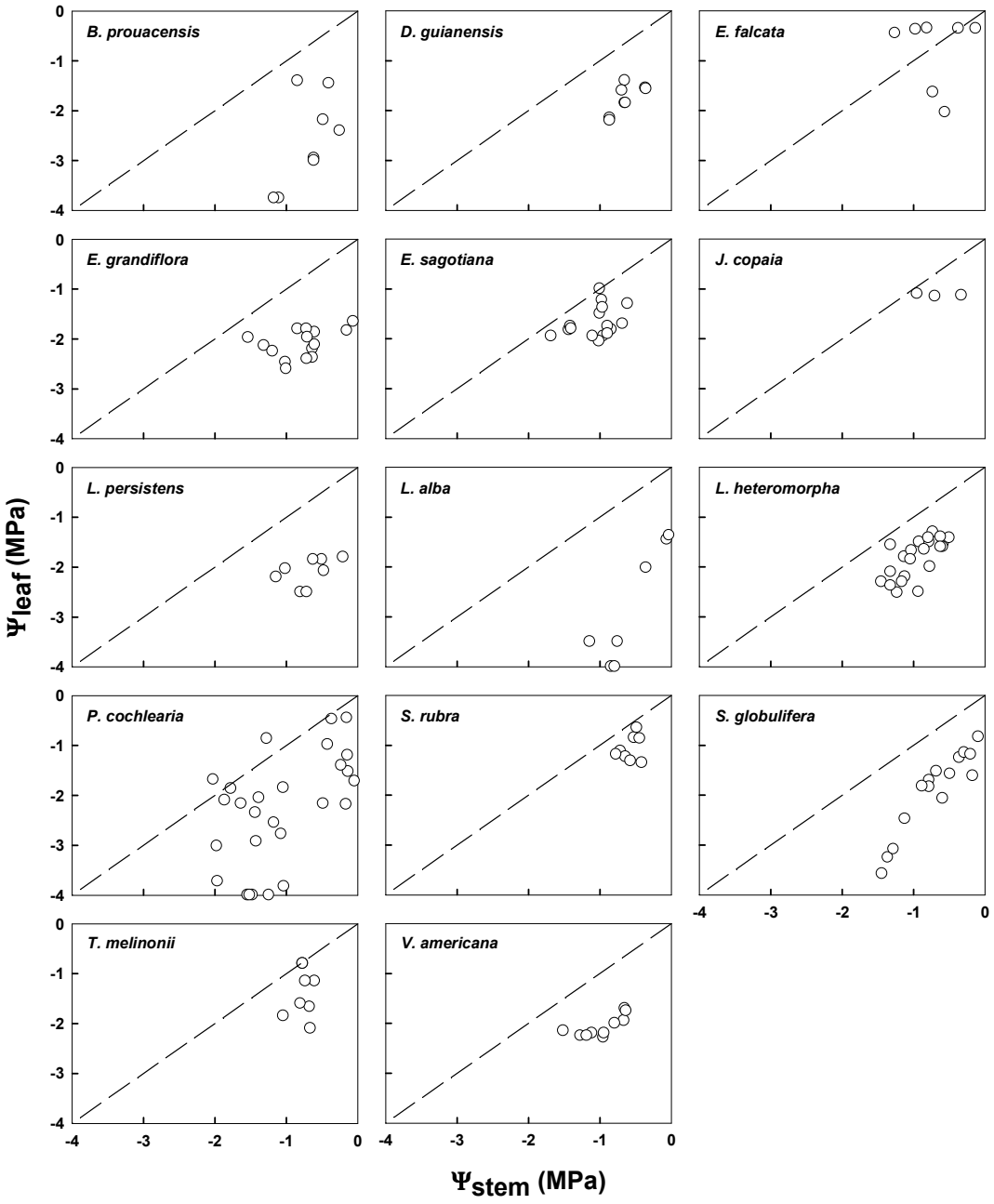

Figure 2.4. Ψ_{leaf} – Ψ_{stem} relationship for 14 Amazonian canopy rainforest tree species sampled from the research plots in French Guiana. The dash line indicates the 1:1 line.

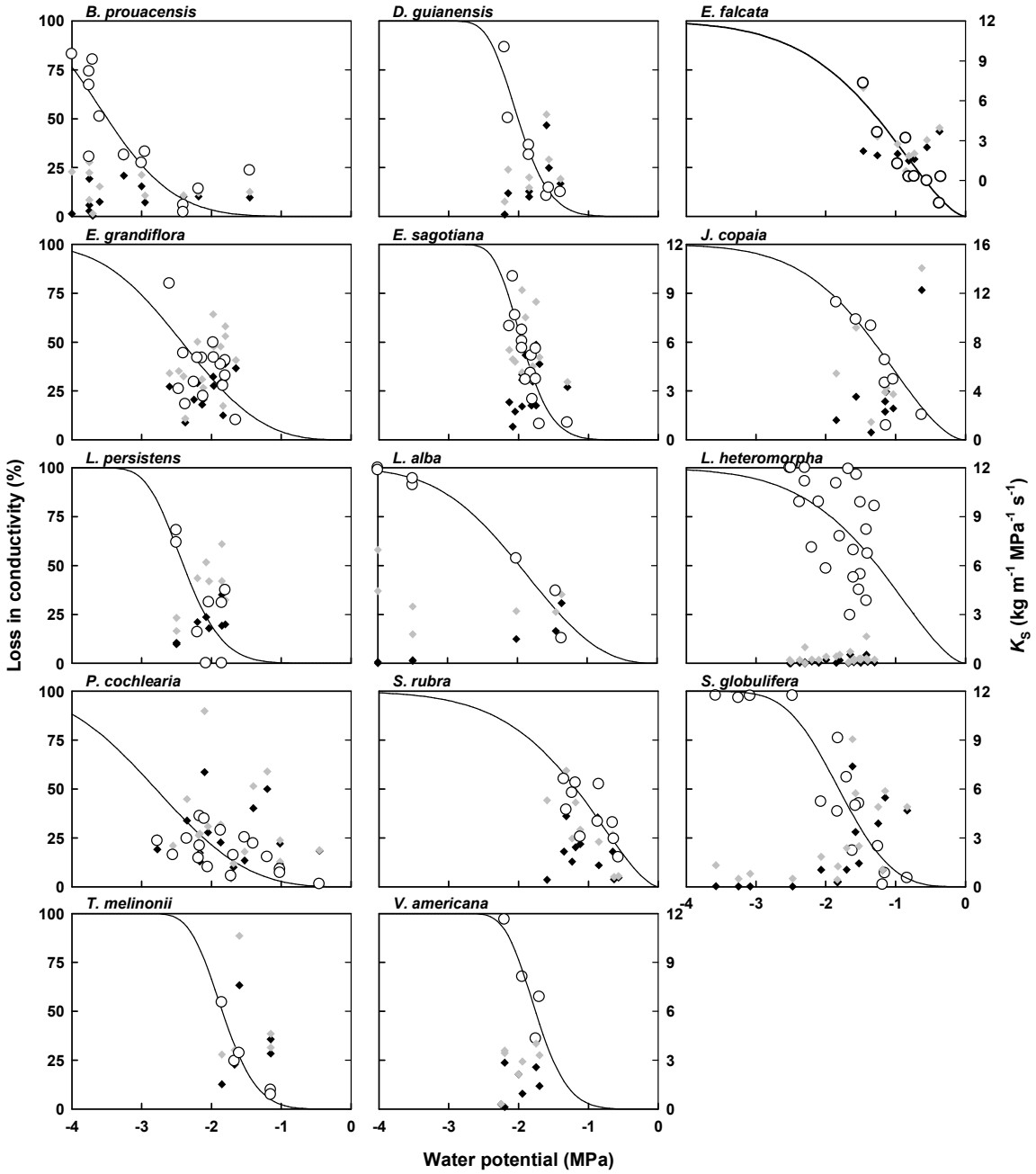

Figure 2.5. Bench top dehydration vulnerability curves of 14 Amazonian canopy rainforest tree species sampled from the research plots in French Guiana. Open circles and solid lines are percent loss in conductivity expressed as Ψ_{leaf} measured after equilibration. Lines are generated using 2-parameter weibull curve fitting. Black diamond are $K_{Snative}$ while the grey diamond are the corresponding K_{Smax}.

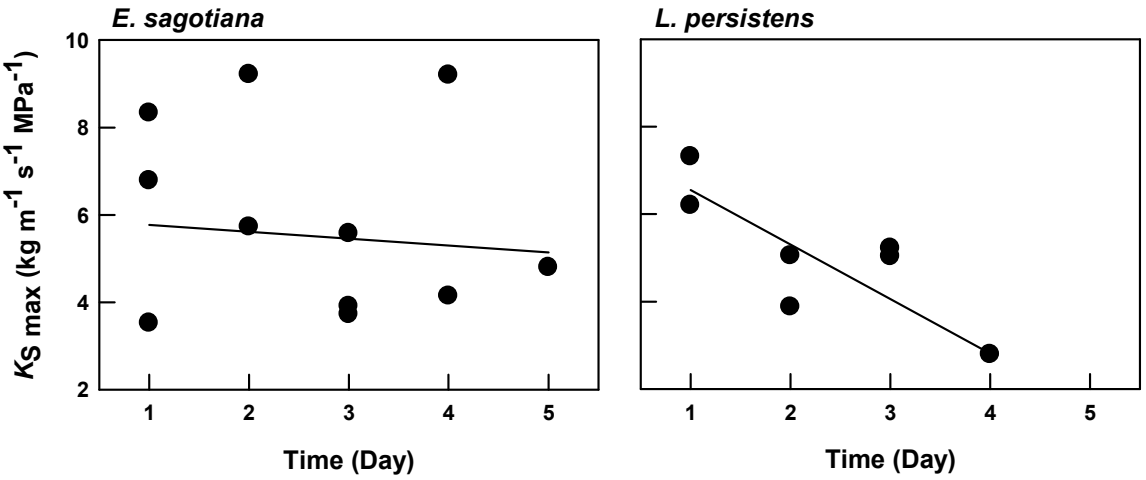

Figure 2.6. Decline of maximum sapwood specific hydraulic conductivity in two Lecythidaceae species. Vessel occlusion is measured as the slope of the line giving the rate of the decline in conductivity.

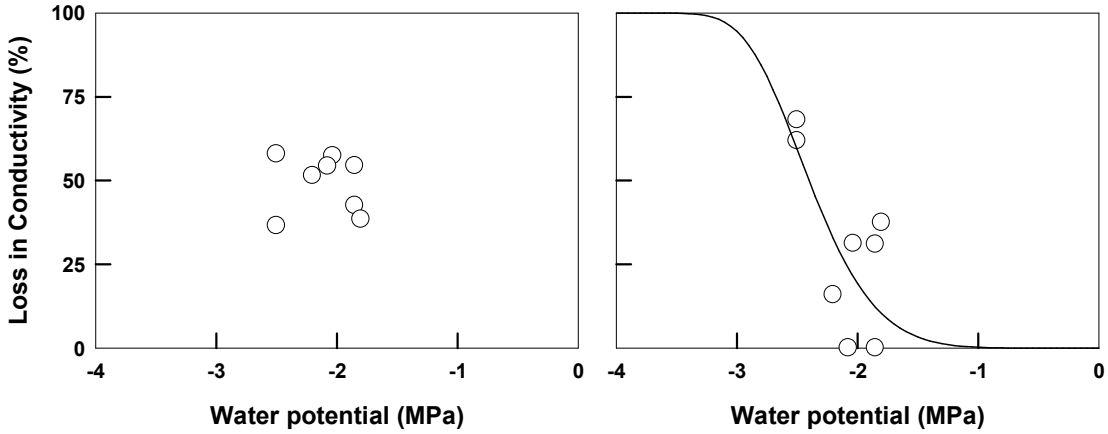

Figure 2.7. Vulnerability curves of *L. persistens* expressed relative to the maximum conductivity of each individual subsamples (*left*) and all subsamples expressed relative to the maximum conductivity on the first day (*right*).

Chapter 3

Photosynthetic and hydraulic physiological performance of three avocado varieties grown under ambient field conditions in a common garden setting.

Abstract

Water is a key resource in agriculture that can negatively impact production when limited. As the amount of resources to produce food dwindle and demand increases, food crops that are able to be productive in low water resource conditions are likely to become increasingly important. We quantified the physiological performance of three avocado varieties *Capa Rosso*, *Criollo*, and *Mantequilla*, grown in a common garden setting under ambient conditions. We evaluated differences in photosynthesis (A_{area}), stomatal conductance (g_s), water use efficiency (*WUE*), carbon ratio between the intercellular portion of leaf and the atmosphere (Ci/Ca), resistance to drought-induced cavitation (P50), cavitation rate (ax), maximum sapwood specific conductivity ($K_{S\,MAX}$), and wood density (ρ_{wood}). No differences were found across the traits measured among varieties except P50, which was found to differ between the *Criollo* and *Mantequilla* varieties. The effectiveness of using plant physiological ecology in methods to identify prospective varieties that are resistant to the effects of drought are discussed.

Introduction

Food production in agriculture is critically tied to the availability of fresh water. Agriculture contributes to roughly 70% of the world's water consumption, which continues to become limited as the world's population continues to increase (Pimentel *et al.*, 1997). With approximately 40% of food produced in irrigated soils (Chaves & Oliveira, 2004), it is crucial to identify ways to increase efficiency in water usage for crops. One of the ways to effectively identify the amount of water needed by crops is to quantify physiological performance and subsequently implement changes in irrigation practices (Blum, 2009). Thus, quantification of crop physiological performance may be useful in informing water use practices in light of the projected changes in climate.

Limitation in water availability exists around the world even without the effects of projected climate scenarios. The projected changes in the rainfall patterns and higher evaporation due to increase in temperature (IPCC, 2012) are likely to intensify the already scarce water supply. These projected changes are already occurring in many parts of the globe. For example, California recently experienced record-breaking drought that placed half of the state in exceptional drought (National Drought Mitigation Center, 2017) and affected water quality and increased water supply costs for food producers throughout the state (USDA ERS, 2017). In the lowland tropics, many tree crop orchards are rain-fed, making them susceptible to short-term drought. In response to the changes in climate patterns, adaptive changes in agriculture are being implemented to mitigate the negative impacts. For example,

farmers across Europe are changing the timing of cultivation and selecting appropriate crop species and cultivars in response to climate change (Olesen *et al.*, 2011). With uncertainty about future water supply, knowledge of the physiological tolerances and optimal performance of crops is crucial to create adaptive implementation.

Physiological processes related to photosynthesis and hydraulic transport influence the amount of carbon and water exchanged between the plant and the atmosphere. Stomatal control in the leaves is one of the way plants are able to control the amount of water lost and the amount of water gained. Control of stomata relative to the environment can result in a significantly increased growth rate (Farquhar & Sharkey, 1982). Furthermore, comparison of the carbon concentration between the atmosphere and the intercellular component of the leaf could give us insight on the effectiveness of carbon diffusion into the plant. Another informative way to quantify the exchange of carbon is by expressing it in relation to the amount of water loss. Expressing water use efficiency (*WUE*) as the amount of carbon gained through photosynthesis per amount of water loss through the stomata reveals how effectively plants can use water. The ability of plants to photosynthesize can be influenced by changes in the amount of water supplied to the photosynthesizing organs by the stem (Santiago *et al.*, 2004a). The amount of water transported through the stem is determined by wood anatomy and density (Zanne *et al.*, 2010) and is also related to the transport strategy (Gleason *et al.*, 2015). Thus, investigating the traits that

describe processes of carbon and water dynamics can present a holistic view of plant performance.

We investigated the physiological performance in relation to photosynthesis and hydraulic transport in an economically important tropical and sub-tropical tree crop *Persea americana* (avocado). The increasing uncertainty in water supply (Olesen *et al.*, 2011) will create difficulties in food production and thus it is important to find crops that are able to perform well physiologically under different environmental thresholds. The objective of the study was to compare the physiological performance of three varieties of avocado grown in the same ambient condition without additional water input. Specifically, we asked if the varieties performed differently in regulating gas exchange for photosynthesis. We explore this question by characterizing the amount of carbon fixed in the leaf and its efficiency in terms of the carbon and water economy between the leaf and the atmosphere. We also asked how the stem performs when supply of water become limited. We addressed this question by characterizing hydraulic conductivity and vulnerability to cavitation of the stems.

Materials and methods

Field site and plant varieties

The study was conducted in variety trial located in the lowlands of Chiriqui, Panama and administered by the federal Panamanian agricultural agency MIDA (Ministerio de Desarrollo Agropecuario – Panamá). The site experienced ca 1900 mm annual precipitation and 28°C mean annual temperature during the study 2012 (World Weather Online, 2017). The soils are composed of clayey, kaolinitic, and isohyperthermic soils that maintain temperature stability throughout the year (Manrique, 2008).

The avocado varieties used for this comparative study were 3-year old *Capa rosso*, *Criollo*, and *Mantequilla* trees grown in a common garden setting spaced 5 m apart under ambient climatic condition devoid of additional irrigation. *Capa rosso* has distinct red tinted leaves that layer the edge of canopy giving it a red hue when seen from a distance. *Criollo* is a landrace variety locally grown throughout Chiriqui and the Caribbean region, with medium leaf size relative to the other varieties. *Mantequilla* is a variety brought from outside Chiriqui and garnered its name due to the buttery flavor of its fruit.

Gas exchange measurements

In August 2012, photosynthetic gas exchange was measured on the youngest fully mature leaves on four individuals per variety using an infrared gas analyzer (LI-6400; LI-COR Biosciences, Lincoln, NE) with a red-blue light source (6400-02B no.

SI-710; LI-COR Biosciences). Measurements were conducted between 0900 h and 1100h. Leaves were clamped with the chamber set with a photon flux density of 1500 μmol m^{-2} s^{-1}. Stable readings were collected for photosynthetic assimilation per area (A_{area}; μmol m^{-2} s^{-1}), stomatal conductance (g_s; mol m^{-2} s^{-1}), intrinsic water use efficiency (WUE; A_{area}/ g_s), and the ratio of intercellular to ambient CO_2 concentration (C_i/C_a).

Stem hydraulic conductivity and vulnerability curves

Terminal branches (1.0 – 1.5m in length) were collected from each individual between 0700 and 0900 h. Cut ends were sealed with parafilm and were sealed inside two layers of opaque plastic bags that contained moist paper towels to prevent further transpiration. The samples were transferred in a camper shell to the Smithsonian Tropical Research Institute (STRI) Earl S. Tupper Facility in Ancon, Panama within 6 h of collection where samples were processed for hydraulic measurements. The samples were cut underwater to 20 cm segments and ends shaved with Teflon coated razor blades to placed in partial vacuum under water overnight to rehydrate.

Rehydrated samples were cut to 14 cm segments and ends shaved with Teflon coated razor blade for determination of the maximum hydraulic conductivity ($K_{H\,MAX}$; kg m s^{-1} MPa^{-1}). Hydraulic conductivity (K_H; kg m s^{-1} MPa^{-1}) was determined by connecting the stem to tubing filled with degassed 20 mM KCl perfusion solution filtered through a 0.1 μm capsule filter (GE Water & Process Technologies, Trevose, PA, USA). The proximal end of the stem was connected to a reservoir that was

elevated to maintain a pressure head below 2 kPa and the distal end was connected to a graduated 1-ml pipette (KIMAX-51; Kimble Chase, Vineland, NJ, USA) to determine the flow rate from changes in volume over time. Samples were allowed to equilibrate before and after measurements to make sure that no passive water uptake occurred.

Xylem vulnerability to cavitation was determined using the standard centrifuge method (Alder *et al.*, 1997), where hydraulic conductivity was measured outside of the centrifuge in between a series of increasingly fast spin speeds that induce increasingly negative pressures. Stem segments were loaded in custom rotor in a refrigerated centrifuge (Sorvall RC-5C; Thermo Fisher Scientific, Waltham, MA, USA) with ends in contact with cosmetic sponges placed in L-shaped reservoirs that contain 20 mM KCl solution. The volumes of the solution in each reservoir were maintained at the same amount to prevent flow during centrifugation. Xylem pressures were induced until > 90% of K_H was lost.

A two-parameter Weibull equation calculated using the cumulative distribution function in Microsoft Excel was used to fit the relationship between K_H and xylem pressures (Fig. 1). The resistance to cavitation was expressed as the 50% loss of conductivity in K_H (P50; MPa) and also as the slope of the line tangent to P50 (ax; kg m^{-1} s^{-1} MPa^{-2}). $K_{H\,MAX}$ was also expressed as sapwood specific area by dividing K_H with the xylem cross sectional area ($K_{S\,MAX}$; kg m^{-1} s^{-1} MPa^{-1}).

Wood density (ρ_{wood}; kg m^{-3}) was determined by dividing dry wood samples with the wet volume of the sample determined using the mass displacement method.

Statistical analysis

The trait values were compared between varieties using ANOVA and Tukey HSD pairwise comparison using R studio version 0.99.903 (RStudio Team, 2015) and R base package (R Core Team, 2016). When necessary, data were transformed to meet the assumptions of ANOVA.

Results

The ambient temperature ranged 30.7 – 36.9 °C and the relative humidity ranged 73.1% - 84.9% during the experiment. Gas exchange values did not differ among the three avocado varieties. The variety *Capa Rosso* exhibited the highest water use efficiency (*WUE*) but it did not differ from the other varieties due to the high variance (Table 3.1). The exchange of gases through stomatal conductance influenced both the high variance of *WUE* more than leaf photosynthesis and also the concentration of carbon relative to the atmosphere, but no differences were found among varieties (Table 3.1)

We observed statistically significant difference among varieties for the drought resistance trait P50 where *Criollo* exhibited xylem more vulnerable to cavitation than *Mantequilla*, but both did not differ statistically from *Capa Rosso* (Table 3.1, Fig. 3.1). No differences were found among varieties in the slope of cavitation, maximum hydraulic conductivity, and wood density.

Discussion

Three avocado varieties were similar in their physiological performance with the exception of drought resistance, where *Mantequilla* exhibited the greatest resistance, *Criollo* exhibited the least resistance, and *Capa Rosso* overlapped with both varieties due to high variability (Fig. 3.1, Table 3.1). The lack of distinct differences among the traits measured could be the result of the wet climatic regime the site experiences. Furthermore, the abundance of water available to each plant could also be the result of how each tree are spaced with about five meters from each other thus reducing the chances of competition for the same resources. However, field conditions do not always remain constant thus it is crucial that we consider how each physiological parameter performs across gradients of environmental conditions in order to have a broader view.

The environmental parameters that exerted the most influence on plant physiological function could be attributed to the field conditions. Temperature is one of the important factors since it influences the leaf-to-air vapor pressure deficit and leaf physiology. For example, seasonally dry field sites can have higher *in situ* maximum carboxylation rate of RuBP and high-temperature carbon compensation point relative to wet evergreen forest in lowland tropical forest of Panamá (Slot & Winter, 2017). Furthermore, some of the physiological relationships such as the positive correlation photosynthesis and Ci/Ca in seasonally dry forest do not hold consistent in wet forest (Slot & Winter, 2017). Another field condition that can influence physiological performance is the nutrient property of the soil. A study that

looked at the global effects of soil on photosynthetic traits revealed that high availability of phosphorous results in lower g_s (Maire *et al.*, 2015). The perspective from long term nutrient fertilization studies indicate that increases in nutrients can also increase the maximum photosynthetic rates and water transport (Santiago, 2015). Both temperature and nutrients directly impact the physiological processes in the plants that results in adjustments such as the ones mentioned above. However, we can also discern that both processes are linked to water because of its direct effect on evaporative cooling and nutrient mobilization.

The latent capacity of plants to utilize an amount of water source can be roughly inferred from wood density. Wood density in plants can vary from low to high across different species and the corresponding mechanical investments therein are tied to the soil where poor nutrient content results in higher mechanical investment (Fortunel *et al.*, 2014; Heineman *et al.*, 2016). Transport capacity by wood is influenced by the structure of its components where the size and number of vessels dictate the volume of sap transported (Zanne *et al.*, 2010). For this reasoning, there is an observed weak trade-off between plants with high conductive capacity and high probability of embolism compared to plants with low conductive capacity that have greater resistance to cavitation (Gleason *et al.*, 2015). From our study we found that there were differences in P50 between two varieties despite the similarity in wood density (Table 1), which suggests slight differences in how the wood is structured. Wood mechanical investment can change with respect to climate. For example, results from a reciprocal transplant across a climate gradient in boreal forest

environment indicate a high phenotypic plasticity of vessel diameter (Schreiber *et al.*, 2015). An experimental manipulation will be needed to discern the phenotypic plasticity of vessel diameter of the avocado varieties in this study.

Determining the capacities of avocado varieties to resist drought can be informative for decisions to determine the varieties to plant in locations with limited water resources. Selecting varieties that are resistant to drought could be advantageous in fields that have high transpirational demands since many tropical tree crop orchards are rain-fed, so drought may not negatively impact the crop physiological performance compared to the less resistant varieties. We could draw inspiration from natural systems for insight on how trees in the forests could manage to grow in many environments despite the environmental limitations. For example, the tropical tree *Cordia alliodora* that spans different neotropical forest types was found to have an advantage due to its ability to adjust drought resistance according to dryness of the sites while maintaining other hydraulic traits such as K_S consistent (Choat *et al.*, 2007). Of the avocado varieties we measured, *Capa Rosso* exhibited the most variation in its resistance to cavitation and thus could become a very good candidate in fields that experience high climatic variation. Thus, quantification of drought resistance gives us the capacity to evaluate crop varieties for drought resistance potential.

Plant physiological ecology is well equipped with tools to address many problems that face agriculture, such as limitation in resources to grow crops. Currently, crop production is highly focused on yields that are achieved by high input

of water and nutrient (Blum, 2009). This form of production depends on the cost of resources. However, the recent droughts in California indicate that the availability of resources are volatile and that in times when such resources are limited, farmers are faced with a choice of either paying a premium to sequester the necessary resource or downsize plant production by irrigating a few trees while leaving the rest to perish from drought. However, alternatives such as finding plants that are water use efficient (Cernusak *et al.*, 2007) can mitigate some of the negative effects of water scarcity.

As we head towards a future where resources to grow crops could become very limiting in food production, incorporating actions that break the current norm can help develop ways of solving critical issues some of which we may have never seen before. Plant physiological ecology has developed tools to quantify how trees are able to perform despite limitations.

References

Alder N, Pockman WT, Sperry JS, Nuismer S. **1997**. Use of centrifugal force in the study of xylem cavitation. *Journal of Experimental Botany* **48**: 665–674.

Blum A. **2009**. Effective use of water (EUW) and not water-use efficiency (WUE) is the target of crop yield improvement under drought stress. *Field Crops Research* **112**: 119–123.

Cernusak LA, Aranda J, Marshall JD, Winter K. **2007**. Large variation in whole-plant water-use efficiency among tropical tree species. *New Phytologist* **173**: 294–305.

Chaves MM, Oliveira MM. **2004**. Mechanisms underlying plant resilience to water deficits: Prospects for water-saving agriculture. *Journal of Experimental Botany* **55**: 2365–2384.

Choat B, Sack L, Holbrook NM. **2007**. Diversity of hydraulic traits in nine *Cordia* species growing in tropical forests with contrasting precipitation. *New Phytologist* **175**: 686–98.

Farquhar GD, Sharkey TD. **1982**. Stomatal Conductance and Photosynthesis. *Annual Review of Plant Physiology* **33**: 317–345.

Fortunel C, Ruelle J, Beauchêne J, Fine PVA, Baraloto C. **2014**. Wood specific gravity and anatomy of branches and roots in 113 Amazonian rainforest tree species across environmental gradients. *New Phytologist* **202**: 79–94.

Gleason SM, Westoby M, Jansen S, Choat B, Hacke UG, Pratt RB, Bhaskar R, Brodribb TJ, Bucci SJ, Cao K, *et al.* 2015. Weak tradeoff between xylem safety and xylem-specific hydraulic efficiency across the world s woody plant species. *New Phytologist* **209**: 123–136.

Heineman KD, Turner BL, Dalling JW. **2016**. Variation in wood nutrients along a tropical soil fertility gradient. *New Phytologist* **211**: 440-454.

IPCC. 2012. Managing the risks of extreme events and disasters to advance climate change adaptation. New York.

Maire V, Wright IJ, Prentice IC, Batjes NH, Bhaskar R, van Bodegom PM, Cornwell WK, Ellsworth D, Niinemets Ü, Ordonez A, *et al*. 2015. Global effects of soil and climate on leaf photosynthetic traits and rates. *Global Ecology and Biogeography* **24**: 706–717.

Manrique LA. **2008**. Effect of extreme soil acidity conditions on plant growth and yield of cassava. *Communications in Soil Science and Plant Analysis* 16: 959–970.

National Drought Mitigation Center. **2017**. US Drought Monitor.

Olesen JE, Trnka M, Kersebaum KC, Skjelvåg AO, Seguin B, Peltonen-Sainio P, Rossi F, Kozyra J, Micale F. **2011**. Impacts and adaptation of European crop production systems to climate change. *European Journal of Agronomy* **34**: 96–112.

Pimentel D, Houser J, Preiss E, White O, Fang H, Mesnick L, Barsky T, Tariche S, Schreck J, Alpert S. **1997**. Water Resources: Agriculture, the Environment, and Society. *BioScience* **47**: 97–106.

R Core Team. **2016**. R: A language and environment for statistical computing.

RStudio Team. **2015**. RStudio: Integrated Development for R.

Santiago LS. **2015**. Nutrient limitation of eco-physiological processes in tropical trees. *Trees* **29**: 1291–1300.

Santiago LS, Goldstein G, Meinzer FC, Fisher JB, Machado K, Woodruff D, Jones T. **2004**. Leaf photosynthetic traits scale with hydraulic conductivity and wood density in Panamanian forest canopy trees. *Oecologia* **140**: 543–550.

Schreiber SG, Hacke UG, Hamann A. **2015**. Variation of xylem vessel diameters across a climate gradient: insight from a reciprocal transplant experiment with a widespread boreal tree. *Functional Ecology* **29**: 1392-1401.

Slot M, Winter K. **2017**. *In situ* temperature response of photosynthesis of 42 tree and liana species in the canopy of two Panamanian lowland tropical forests with contrasting rainfall regimes. *New Phytologist* **214**: 1103-1117.

USDA ERS. **2017**. California Drought: Farms.

World Weather Online. **2017**. Chiriqui, Panama weather.

Zanne AE, Westoby M, Falster DS, Ackerly DD, Loarie SR, Arnold SEJ, Coomes DA. **2010**. Angiosperm wood structure: Global patterns in vessel anatomy and their relation to wood density and potential conductivity. *American Journal of Botany* **97**: 207–15.

Tables and Figures

Table 3.1. Summary of traits for the avocado varieties. The values are reported as mean ± SE. Test statistics reported are from ANOVA. Tukey HSD pairwise comparisons indicated by superscript letters are reported only for significant statistical results.

Traits	Capa Rosso	Criollo	Mantequilla	Test Statistic	P-Value
A_{area}(μmol m^{-2} s^{-1})	24.5 ± 1.9	20.8 ± 2.5	19.2 ± 2.7	1.31	0.32
g_s (mol m^{-2} s^{-1})	0.176 ± 0.017	0.276 ± 0.098	0.335 ± 0.066	1.27	0.33
WUE (μmol mol^{-1})	182.7 ± 54.9	54.46 ± 28.1	64.44 ± 6.84	2.77	0.14
Ci/Ca	0.446 ± 0.035	0.768 ± 0.23	0.716 ± 0.027	2.26	0.17
P50 (MPa)	-0.63 ± 0.14^{A,B}	-0.38 ± 0.053^{A}	-0.86 ± 0.10^{B}	4.89	0.041
ax (kg m^{-1} s^{-1} MPa^{-2})	1.46 ± 0.10	1.38 ± 0.099	1.87 ± 0.43	1.36	0.31
$K_{S\ MAX}$ (kg m^{-1} s^{-1} MPa^{-1})	4.81 ± 0.45	6.87 ± 0.61	4.79 ± 0.87	3.75	0.071
ρ_{wood} (kg m^{-3})	390.8 ± 26.7	391.5 ± 12.7	372.4 ± 31.6	0.186	0.83

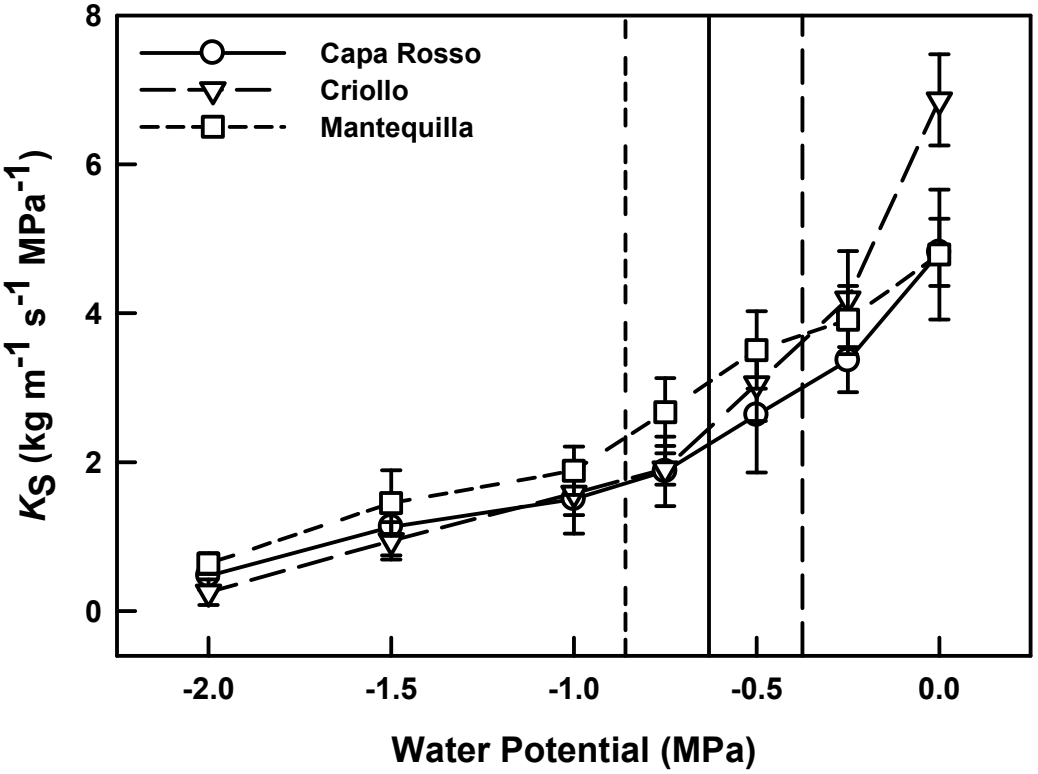

Figure 3.1. The decline in hydraulic conductivity of the avocado varieties versus the decrease in the xylem pressure. The vertical lines indicate the 50 percent loss in conductivity for each of the variety. The symbols represent the mean hydraulic conductivity value for the corresponding xylem pressure and the bars represent one standard error.

Conclusion

There are three main messages from this dissertation. First, the diversity of species in tropical forest also translates to the hydraulic strategies employed by canopy plants. Second, compared to the global distribution of hydraulic traits (Gleason *et al.*, 2015), tropical woody plants utilize traits that maximize water usage more than drought resistance as evident from the narrower range in vulnerability to cavitation compared to capacitance and hydraulic conductivity. These were evident from values reported for capacitance and hydraulic transport from the studies in both the first and second chapters. Third, the knowledge we learn from and methods we develop to study natural systems can greatly inform our understanding of crop performance as evident from the third chapter.

Hydraulic strategies were the common concept that spanned across the chapters in the dissertation. It is becoming clear that in tropical systems multiple hydraulic traits are needed in order to fully characterize the contributions of woody plants to the hydrological cycle. To date, only plant hydraulic strategies relative to drought traits have been investigated (Choat *et al.*, 2012) which gave us an insight on global convergence of drought vulnerability. However, insights from global dataset also revealed that there are also other dimensions in plant hydraulic strategies since the current framework based on safety-efficiency trade-off is significantly but also only weakly supported (Gleason *et al.*, 2015). This dissertation showcased the importance of avoidance via high coordination among non-drought tolerance hydraulic traits, thus investigating these traits is of

importance in order to identify other dimensions that captures the variation in hydraulic trait axes.

There are multiple avenues to expand the research from this dissertation. Due to the high diversity in tropical forest and also the difficulties in quantifying these traits, it is crucial that more species be quantified for these traits. This includes species that occur in the lowland forests and also the species that occur across many other environmental gradients where tropical forests occur, such as elevation, precipitation, and soil type gradients. Investigating active adjustments in hydraulic transport in light of drought, such as vessel occlusion are crucial, as it seems to span across many lineages (Chattaway, 1949).

References

Chattaway MM. **1949**. The development of tyloses and secretion of gum in heartwood formation. *Australian Journal of Sicentific Research, Series B, Biological Sciences* **2**: 227–249.

Choat B, Jansen S, Brodribb TJ, Cochard H, Delzon S, Bhaskar R, Bucci SJ, Feild TS, Gleason SM, Hacke UG, *et al.* 2012. Global convergence in the vulnerability of forests to drought. *Nature* **491**: 752–5.

Gleason SM, Westoby M, Jansen S, Choat B, Hacke UG, Pratt RB, Bhaskar R, Brodribb TJ, Bucci SJ, Cao K, *et al.* 2015. Weak tradeoff between xylem safety and xylem-specific hydraulic efficiency across the world s woody plant species. *New Phytologist* **209**: 123–136.